



## Synthesis, characterization, and biological studies of diosgenyl analogs

Bao-Zhan Huang, Guang Xin, Li-Mei Ma, Ze-Liang Wei, Yan Shen, Rui Zhang, Hua-Jie Zheng, Xiang-Hua Zhang, Hai Niu & Wen Huang

To cite this article: Bao-Zhan Huang, Guang Xin, Li-Mei Ma, Ze-Liang Wei, Yan Shen, Rui Zhang, Hua-Jie Zheng, Xiang-Hua Zhang, Hai Niu & Wen Huang (2016): Synthesis, characterization, and biological studies of diosgenyl analogs, Journal of Asian Natural Products Research, DOI: 10.1080/10286020.2016.1202240

To link to this article: <http://dx.doi.org/10.1080/10286020.2016.1202240>

 View supplementary material 

 Published online: 05 Jul 2016.

 Submit your article to this journal 

 Article views: 15

 View related articles 

 View Crossmark data 



## Synthesis, characterization, and biological studies of diosgenyl analogs

Bao-Zhan Huang<sup>a</sup>, Guang Xin<sup>a</sup>, Li-Mei Ma<sup>a,b</sup>, Ze-Liang Wei<sup>a</sup>, Yan Shen<sup>a,b</sup>, Rui Zhang<sup>a,b</sup>, Hua-Jie Zheng<sup>a,c</sup>, Xiang-Hua Zhang<sup>a,d</sup>, Hai Niu<sup>a,e</sup> and Wen Huang<sup>a,b,c</sup>

<sup>a</sup>Laboratory of Ethnopharmacology, Institute for Nanobiomedical Technology and Membrane Biology, West China Hospital, Sichuan University, Chengdu 610041, China; <sup>b</sup>Regenerative Medicine Research Center, West China Hospital, Sichuan University, Chengdu 610041, China; <sup>c</sup>Department of Integrated Traditional Chinese and Western Medicine, West China Hospital, Sichuan University, Chengdu 610041, China; <sup>d</sup>Institute of Sort Science, Sichuan University, Chengdu 610041, China; <sup>e</sup>College of Mathematics, Sichuan University, Chengdu 610041, China

### ABSTRACT

A series of diosgenyl analogs were prepared from diosgenin to evaluate their anticancer activity and antithrombotic property. Analog **4**, which had a spiroketal structure with a 6-aminohexanoic acid residue, exhibited the highest potency against all five tumor cell lines. It significantly blocked tumor growth, induced cell apoptosis and autophagy, and regulated cellular calcium concentration, mitochondrial membrane potential, adenosine triphosphate, and cell cycle. In addition, fluorescence-tagged compounds indicated that the analogs could rapidly accumulate in the cytoplasm, but no specific localization in the nucleus of cancer cells was observed. Furthermore, preliminary structure–activity relationship studies demonstrated that spiroketal analogs exhibit better antithrombotic activity than furostanoic analogs, which exhibit the opposite effect by promoting thrombosis. Our study indicates that compound **4** may be a promising anticancer drug candidate for cancer patients with thromboembolism.

### ARTICLE HISTORY

Received 4 March 2016  
Accepted 13 June 2016

### KEYWORDS

Diosgenin; diosgenyl analog;  
antitumor; antithrombosis

## 1. Introduction

Because of its increasing incidence and mortality rate, cancer poses one of the most serious challenges to public healthcare systems and places a huge burden on economic and social development [1]. The World Health Organization attributed 8.2 million deaths to cancer in 2012. Within the next 20 years, the number of new cases of cancer is expected to increase from 14 million in 2012 to as many as 22 million worldwide [2]. Symptomatic thrombosis is a common complication of cancer. Patients with malignancies may have a seven-fold increased risk of developing venous thromboembolism compared to those without cancer [3]. Today, thromboembolism is the second most common cause of death in cancer patients; it accounts for increased morbidity, mortality, and health care costs [4]. Therefore, the

**CONTACT** Wen Huang baozhan2006@163.com

Supplemental data for this article can be accessed <http://dx.doi.org/10.1080/10286020.2016.1202240>.



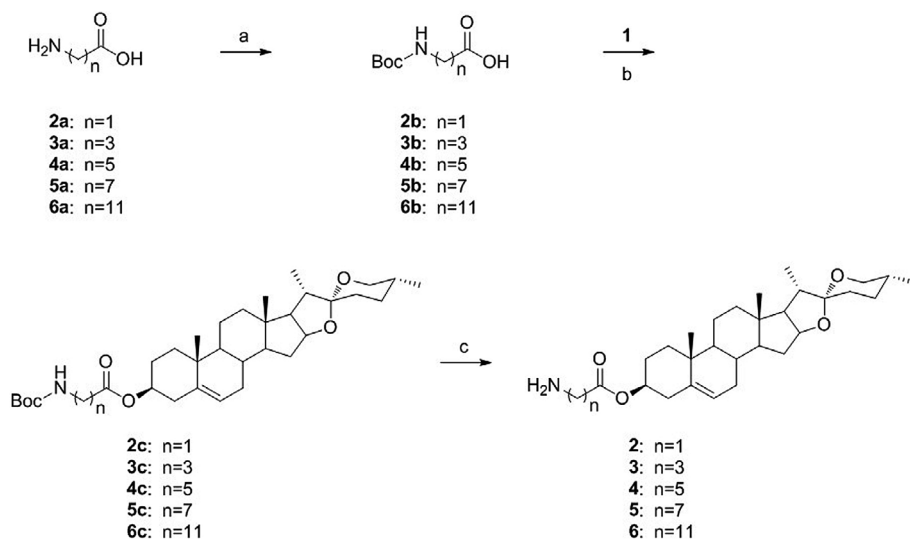
## 2. Results and discussion

### 2.1. Preparation of diosgenyl analogs

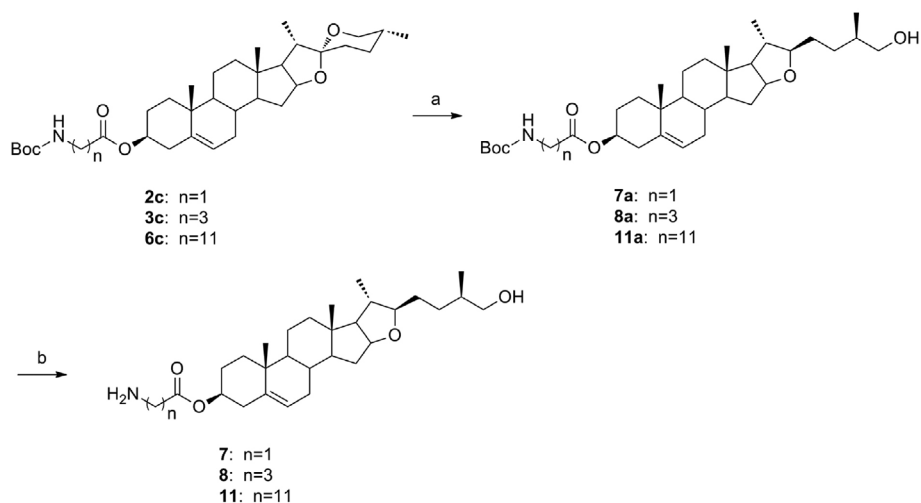
In the present study, a series of straight-chain amino acid diosgenyl esters **2–6** (S-A-1) with straight-chain amino acids containing 2–12 carbon atoms were synthesized in good yields according to the previously reported methods with some modifications (Scheme 1) [13]. Amino acid diosgenyl esters **2–6** were prepared by an esterification reaction involving 1-ethyl-3-(3-dimethylaminopropyl)carbodiimide hydrochloride/4-dimethylaminophenol (EDC-HCl/DMAP), diosgenin, and the corresponding *N*-tert-butoxycarbonyl amino acids in anhydrous dichloromethane. All *N*-protected amino acids **2b–6b** used were synthesized via the reaction of amino acids with di-*tert*-butyl pyrocarbonate ((Boc)<sub>2</sub>O) in acetone–water mixed solvents in the presence of triethylamine (Et<sub>3</sub>N), except for the commercially obtained compound **2b**.

Scheme 2 shows the synthetic strategy of diosgenyl derivatives with furostane skeleton structures starting with diosgenin. Similar to the study by Hamid et al., the F-ring of the spiroketal bond was opened under mild reductive cleavage conditions using sodium cyanoborohydride in acetic acid at room temperature [7]. Compounds **2c–6c** were converted to **7a–11a**, which possess furostane skeleton structures. Then, new straight-chain amino acid diosgenyl derivatives **7, 8, and 11** (S-B) were obtained by deprotection of the *N*-tert-butoxycarbonyl group using trifluoroacetic acid at room temperature.

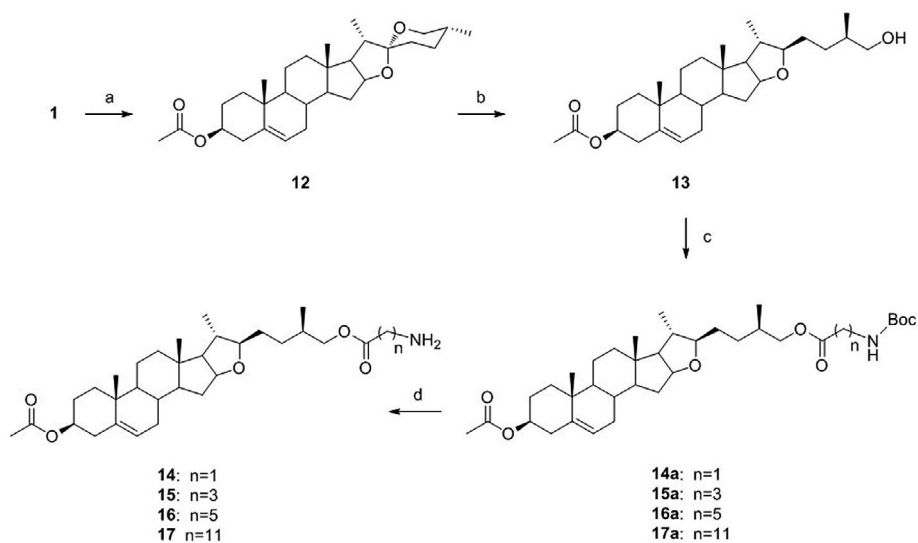
As part of our ongoing research program, diosgenin was acetylated with acetic anhydride–pyridine to yield diosgenyl acetate **12**, and the F-ring of spiroketal linkage was reduced according to the above method to yield a primary alcohol **13**. The alcohol **13** was esterified with four different straight-chain amino acids in the presence of EDC-HCl/DMAP in dry dichloromethane. Finally, the corresponding straight-chain amino acid diosgenyl analogs **14–17** (S-C) were obtained by treating the compounds with trifluoroacetic acid in dichloromethane (Scheme 3).



**Scheme 1.** Synthesis of compounds **2–6**. Reagents and conditions: (a) (Boc)<sub>2</sub>O, Et<sub>3</sub>N, CH<sub>3</sub>COCH<sub>3</sub>–H<sub>2</sub>O (v:v 1:1), rt, 3–6 h, 93%–95%; (b) EDC-HCl, DMAP, CH<sub>2</sub>Cl<sub>2</sub>, 30–35 °C, 4–8 h, 77–82%; (c) CF<sub>3</sub>COOH, CH<sub>2</sub>Cl<sub>2</sub>, 30–35 °C, 2–6 h, 80–87%.

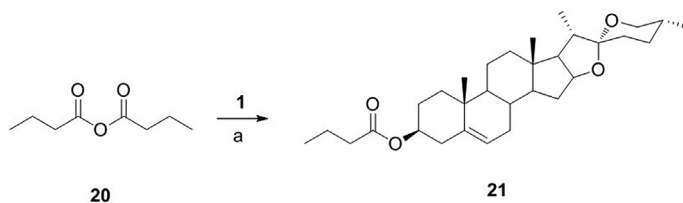


**Scheme 2.** Synthesis of compounds 7–11. Reagents and conditions: (a)  $\text{CH}_2\text{Cl}_2$ ,  $\text{CH}_3\text{COOH}$ ,  $\text{NaBH}_3\text{CN}$ , rt, 16–20 h, 79–85%; (b)  $\text{CF}_3\text{COOH}$ ,  $\text{CH}_2\text{Cl}_2$ , 30–35 °C, 2–6 h, 75–82%.

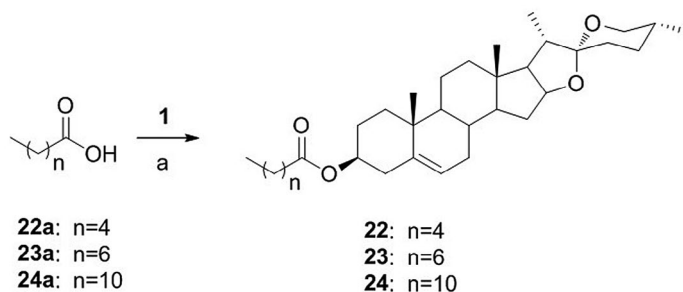


**Scheme 3.** Synthesis of compounds 14–17. Reagents and conditions: (a)  $\text{Ac}_2\text{O}$ , Py, 60 °C, 1 h, 93%; (b)  $\text{NaBH}_3\text{CN}$ ,  $\text{CH}_2\text{Cl}_2$ ,  $\text{CH}_3\text{COOH}$ , rt, 18 h, 85%; (c) EDC-HCl, DMAP,  $\text{CH}_2\text{Cl}_2$ , 30–35 °C, 3–8 h, 79–88%; (d)  $\text{CF}_3\text{COOH}$ ,  $\text{CH}_2\text{Cl}_2$ , 30–35 °C, 2–6 h, 86–92%.

To further evaluate the antitumor effect of the primary amine of straight-chain amino acid diosgenyl esters, another four straight-chain fatty acid diosgenyl esters **21–24** (S-A-2) without primary amine residues were designed and synthesized with diosgenin as the starting material. Compound **21** was obtained by acetylation with diosgenin, butyric anhydride, and pyridine at room temperature (Scheme 4). Fatty acid diosgenyl esters **22–24**



**Scheme 4.** Synthesis of compound 21. Reagents and conditions: (a) butyric anhydride, pyridine, rt, 7 h, 89%.



**Scheme 5.** Synthesis of compounds 22–24. Reagents and conditions: (a) EDC-HCl, DMAP,  $\text{CH}_2\text{Cl}_2$ , 30–35 °C, 2–6 h, 79–84%.

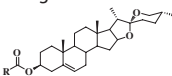
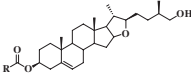
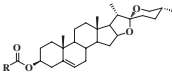
were prepared by an esterification reaction involving EDC-HCl/DMAP, diosgenin, and the corresponding straight-chain fatty acids in anhydrous dichloromethane (Scheme 5).

## 2.2. Structure–activity relationship of diosgenyl analogs against tumor cells

In this work, diosgenyl analogs, including five straight-chain amino acid (22 $\beta$ , 25R)-spirost-5-en-3 $\beta$ -yl esters (2–6) (S-A-1), three straight-chain amino acid (25R)-furost-5-en-26-ol-3 $\beta$ -yl esters (7, 8 and 11) (S-B), four straight-chain amino acid (25R)-furost-5-en-3 $\beta$ -acetoxy-26-yl esters (14–17) (S-C), and five straight-chain fatty acid (22 $\beta$ , 25R)-spirost-5-en-3 $\beta$ -yl esters (12, 21–24) (S-A-2) were synthesized and the cytotoxic activity of these compounds was evaluated through the 3-(4,5-dimethyl-2-thiazolyl)-2,5-diphenyl-2-H-tetrazolium bromide (MTT) assay in the following tumor cell lines: murine colon carcinoma C26 cells, mouse melanoma B16 cells, human hepatocellular carcinoma HepG2 cells, human lung carcinoma A549 cells, and human breast cancer MDA-MB-231 cells. The  $\text{IC}_{50}$  values of deltonin were also included in the study for comparison.

The data presented in Table 1 show that compounds 3–5 (S-A-1) and compound 8 (S-B), which have straight-chain amino acid side chains with a 4–8 carbon chain length, demonstrate significantly higher inhibitory activity against all five cancer cell lines than either diosgenin or other diosgenyl analogs that have straight-chain amino acid side chains with a too short or long carbon chain length (e.g. 2 or 12 carbon atoms). Among them, compound 4 containing a 6-aminocaproic acid residue with 6-carbon atom length shows

**Table 1.** *In vitro* antiproliferative activities of diosgenyl analogues.<sup>a</sup>

Compound		IC <sub>50</sub> (μM)				
		C26	B16	HepG2	A549	MDA-MB-231
1	Diosgenin	> 30	> 30	> 30	> 30	> 30
2		> 30	> 30	> 30	> 30	> 30
3	(S-A-1)	7.7 ± 0.8	12.3 ± 2.4	28.5 ± 4.3	12.2 ± 1.6	10.1 ± 0.6
4		5.5 ± 0.6	8.6 ± 1.0	16.9 ± 2.1	13.4 ± 2.6	8.3 ± 1.2
5	R=	8.9 ± 0.8	10.6 ± 1.2	20.8 ± 2.7	17.8 ± 2.9	13.0 ± 1.5
6		> 30	> 30	> 30	> 30	> 30
7		> 30	> 30	> 30	> 30	> 30
8	(S-B)	9.4 ± 0.7	8.8 ± 1.7	> 30	10.7 ± 1.1	14.4 ± 1.3
11		> 30	> 30	> 30	> 30	> 30
14	R=	> 30	> 30	> 30	> 30	> 30
15	(S-C)	22.3 ± 0.6	> 30	> 30	> 30	> 30
16		25.7 ± 3.8	> 30	> 30	> 30	> 30
17		> 30	> 30	> 30	> 30	> 30
12	R=	> 30	> 30	> 30	> 30	> 30
12		> 30	> 30	> 30	> 30	> 30
21	(S-A-2)	> 30	> 30	> 30	> 30	> 30
22		> 30	> 30	> 30	> 30	> 30
23		> 30	> 30	> 30	> 30	> 30
24	R=	> 30	> 30	> 30	> 30	> 30
28		> 30	> 30	> 30	> 30	> 30
35		10.4 ± 2.6	15.3 ± 2.7	23.5 ± 2.6	16.4 ± 1.8	15.4 ± 2.2
Deltonin <sup>b</sup>		2.3 ± 0.7	5.6 ± 1.3	8.8 ± 2.1	8.6 ± 1.4	3.5 ± 0.7

<sup>a</sup>Data are obtained from a minimum of  $n = 3$  independent MTT assays for each compound, and represented as mean ± s.e.m.

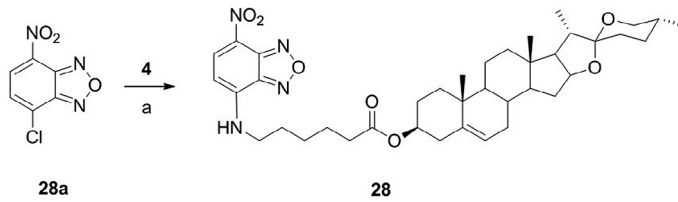
<sup>b</sup>Deltonin was used in the study for comparison.

stronger activity than other diosgenyl analogs, especially compound **4** against C26 cell lines (IC<sub>50</sub> 5.5 μM). It may be noted that straight-chain amino acid diosgenyl analogs with S-A-1 and S-B structures have better activity than those with S-C structures. Amino acid diosgenyl analogs **2–6** (S-A-1) exhibited higher anticancer activity than highly lipophilic fatty acid diosgenyl analogs **12**, **21–24** (S-A-2), which do not have a primary amino group. These results suggest that the 4–8 carbon chain length of straight-chain amino acid residues and S-A-1 and S-B aglycon structures are optimal for the antitumor effect of diosgenyl analogs.

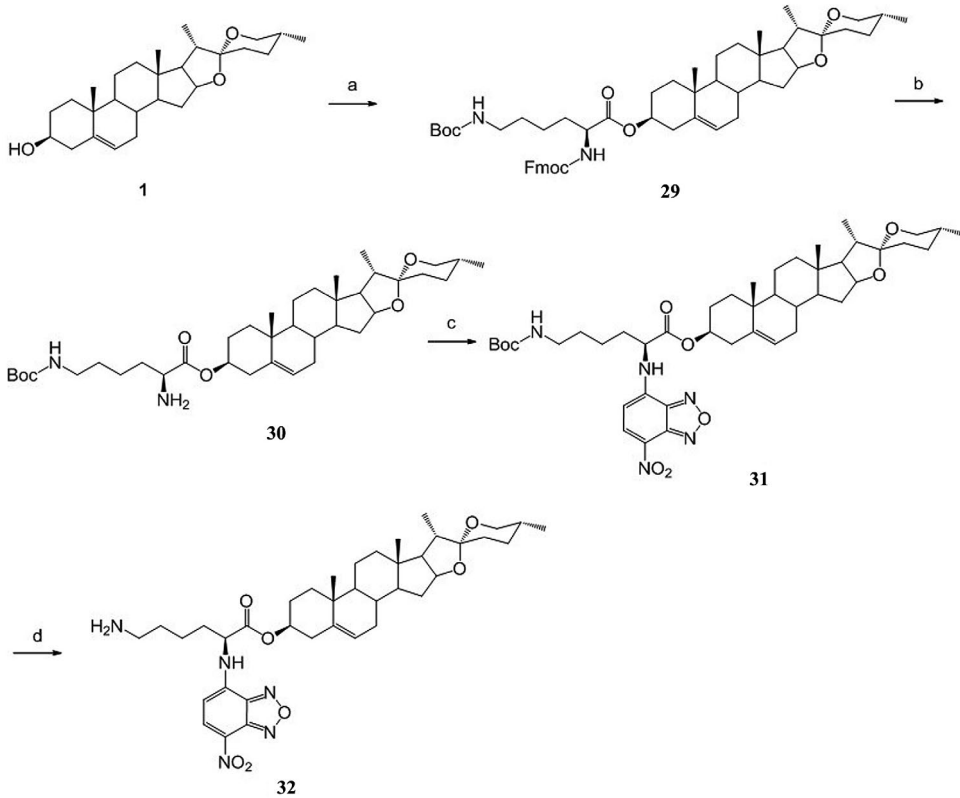
### 2.3. Fluorescent cell imaging and cellular distribution of diosgenyl analogs

Increasing pre-clinical and mechanistic studies had been independently conducted and showed that diosgenin and diosgenyl derivatives exhibited antiproliferative effects against several types of cancer via multiple molecular mechanisms [9,10]. However, the mechanisms of action of these molecules against tumors remained unclear, and there was little information available on the localization and distribution of these molecules in live cells.

Fluorescence imaging of the living cells would be the most powerful means for the real-time monitoring of cellular processes (including specific interactions or subcellular



**Scheme 6.** Synthesis of compound **28**. Reagents and conditions: (a) NBD-Cl, Et<sub>3</sub>N, THF, 50 °C, 5 h, 66%.



**Scheme 7.** Synthesis of compound **32**. Reagents and conditions: (a) *N*- $\alpha$ -Fmoc-*N*- $\epsilon$ -Boc-L-lysine, EDC-HCl, DMAP, CH<sub>2</sub>Cl<sub>2</sub>, rt, 18 h; (b) piperidine, DMF, rt, 3 h; (c) NBD-Cl, Et<sub>3</sub>N, THF, 50 °C, 4 h; (d) CF<sub>3</sub>COOH, CH<sub>2</sub>Cl<sub>2</sub>, 30 °C, 4 h.

localization) of bioactive molecules [20]. Reported protocols for the fluorescence-tagged natural products are tedious and result in low yield because of laborious reaction steps and protection–deprotection procedures. The molecular sizes of the fluorescent probes, such as fluorescein and rhodamine, are usually too large and may induce alterations in membrane organization [20]. It has been reported that 4-chloro-7-nitrobenz-2-oxa-1,3-diazole (NBD-Cl) is nonfluorescent, small in size, has high permeability, and easily undergoes nucleophilic substitution by the amine functional group to become a highly sensitive

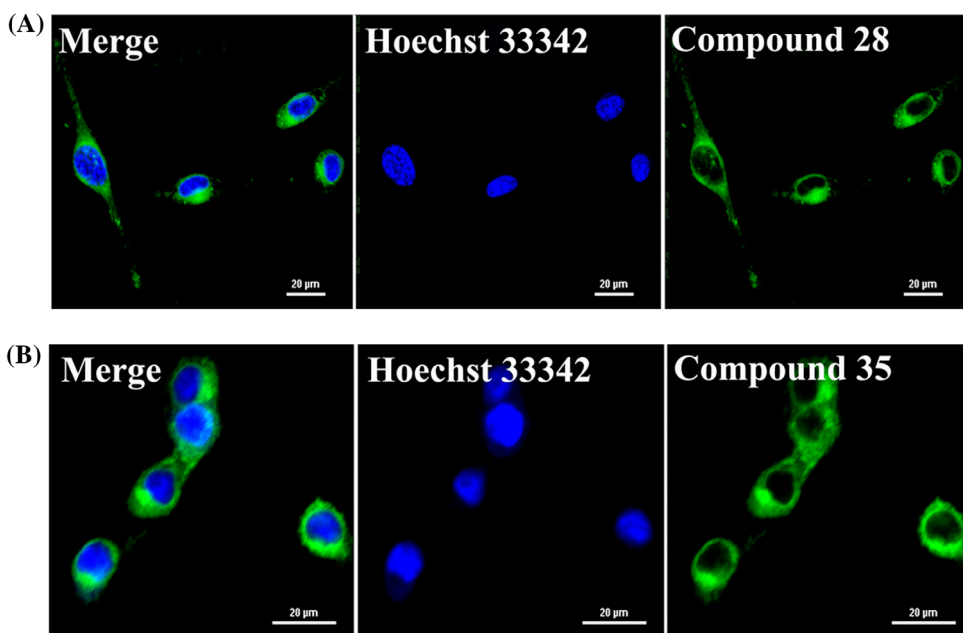


**Figure 2.** The cellular localization of diosgenyl analogues in live C26 cells.

Notes: C26 cells were incubated with 10  $\mu\text{M}$  compound **28** (A) and compound **35** (B) for 24 h, co-stained with Hoechst 33,342, and then imaged using a laser scanning confocal microscopy. Nucleus: blue (Hoechst 33,342), cytoplasm: green (NBD-labeled diosgenyl analogues).

fluorescent entity [20]. Therefore, NBD-Cl is a good tag to label bioactive compounds, and can be applied to track their mode of action through fluorescent cell imaging.

Here, NBD-Cl was successfully used to label diosgenyl analogs, and two NBD-tagged diosgenyl derivatives **28** and **32** were synthesized in high yield (Schemes 6 and 7). C26 cells were treated with compounds **28** and **32** (10  $\mu\text{M}$ ) for 24 h, and analyzed for cellular internalization and localization under a confocal microscope. Our data illustrated that compounds **28** and **32** localized and played a role in the plasma membrane and cytoplasm of C26 cells, but no specific localization in the nucleus was seen (Figure 2). Then, the cytotoxic activity of these two compounds was evaluated through an MTT assay. Compounds **32** and **4**, both containing a primary amino group, exhibited equal anticancer activity, and showed higher inhibition against cancer cells than compound **28**, which lacks a primary amino group (Table 1).

The labeling of small molecules with fluorescent probes is an attractive technique to elucidate cellular processes, and it has gradually become a trend in cell biology that this technique was used to investigate the location of the bioactive molecules. Evaluation of the cytotoxic activity of NBD-tagged diosgenyl derivative **32** and diosgenyl analog **4** indicated that the labeling of NBD residues did not drastically alter the cytotoxic activity. The internalization and localization of diosgenyl analogs were imaged successfully inside the C26 cells. The analogs were found to be localized in the plasma membrane and cytoplasm but not in the nucleus. In addition, NBD-based fluorescent labeling protocol works well under mild conditions. Therefore, this methodology can be applied for other diosgenyl

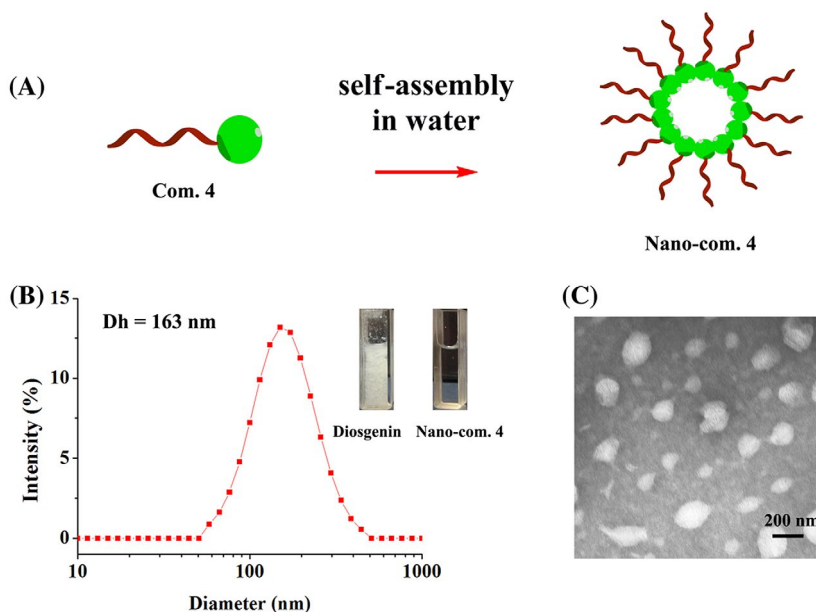


**Figure 3.** Diameter distribution of nanocompound **4** in ethanol–water solution. (A) Schematic illustration of compound **4** self-assembled into nanoparticles in 2% ethanol–water solution. (B) Diameter distribution of compound **4** in 2% ethanol–water solution, and the average size ( $D_h$ ) was 163 nm. Inset: digital photographs of diosgenin (1 mg/ml) and nano-compound **4** (1 mg/ml) in 2% ethanol–water solution. (C) TEM image of compound **4** nanoparticles in 2% ethanol–water solution.

derivatives and even natural saponins to study cellular processes, especially cellular uptake, distribution, or specific interactions.

#### 2.4. The antitumor effect of analogue **4** *in vivo* and *in vitro*

Clinical application of diosgenin and its analogs in cancer therapy is limited due to their undesirable pharmaceutical characteristics, such as poor solubility and low bioavailability [21]. Nanotechnology for drug delivery can improve pharmacokinetics, prolong the sustain release of drugs, and preferentially accumulate in tumor by the enhanced permeability and retention effect [2,21]. Here, the amphiphilic analog **4** (5 mg) was dissolved in the ethanol (100  $\mu$ l), and then slowly added into deionized water (5 ml) under stirring. Compound **4** (1 mg/ml) was soluble in 2% ethanol–water solution, while diosgenin was insoluble at the same concentration in 2% ethanol–water solution (Figure 3(A) and (B)). Surprisingly, we found that compound **4** could successfully self-assemble into nanoparticles in water because of its amphiphilic property (Figure 3(A)–(C)). Using nanoparticle size analyzer (DSA) and transmission electron microscope (TEM), the mean hydrodynamic diameter size was about 163 nm with a unimodal size distribution (Figure 3 (B) and (C)). The nanodrug delivery system of the diosgenyl analogue may attribute to its antitumor property.

In this study, compound **4**, the most potent molecule of the series, was selected to further elucidate the molecular mechanism of action of diosgenyl analogs against cancer *in vitro* and *in vivo*. To determine the cytotoxicity of compound **4** in C26 cells, cells were treated

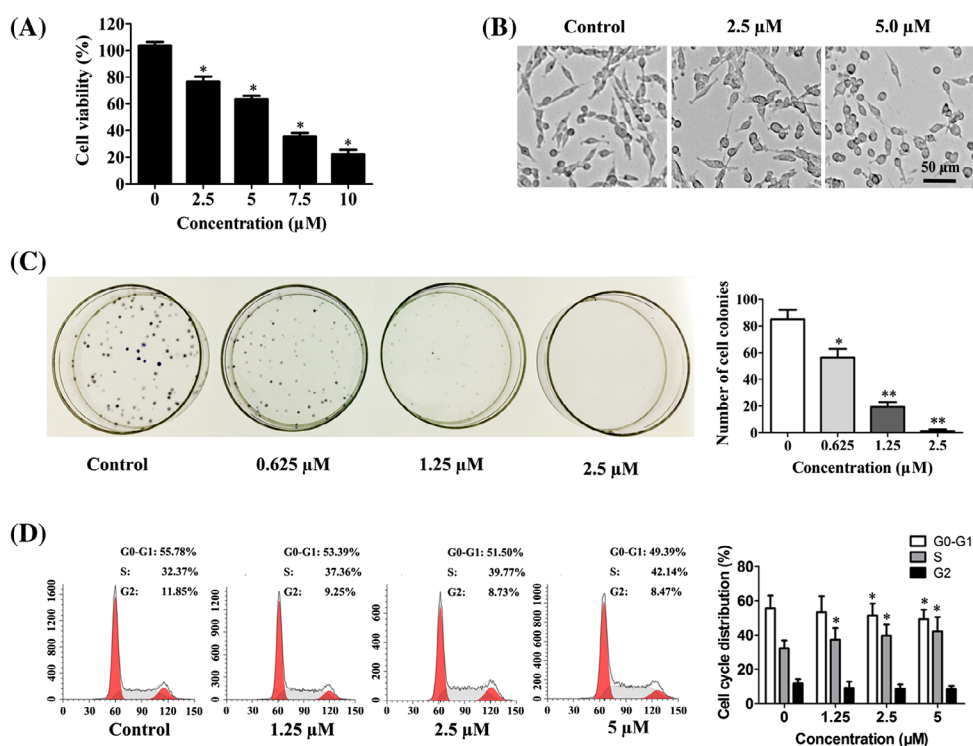


**Figure 4.** The growth inhibition of C26 cells treated with compound 4 *in vitro*. (A) Compound 4 blocked C26 cells growth in a dose-dependent manner. (B) Compound 4 inhibited C26 cells proliferation and induced cell morphology changes. (C) Compound 4 suppressed C26 cell colonies formation in a dose-dependent manner. (D) Compound 4 blocked C26 cell cycle arrest in S phase.

Note: \* $p < 0.05$ ,  $p < 0.01$  compared to control, error bars depict s.e.m.

with different concentrations of compound 4. Our data showed that compound 4 could effectively inhibit cell proliferation (Figure 4(A)). Furthermore, results from microscopic images of cell morphology showed that significant cell death was observed after treatment with compound 4 for 24 h (Figure 4(B)). In addition, compound 4 significantly blocked C26 cell colony formation in a dose-dependent manner (Figure 4(C)). Cell cycle regulation assures the fidelity of cell division and genomic replication. Induction of cell cycle arrest in cancer cell lines leads to genomic instability, which is one of the most prevalent strategies to stop cancer from spreading. Our data demonstrated that compound 4 arrested cancer cells in S-phase to block DNA replication and induce cell death (Figure 4(D)).

In addition, compound 4 led to intracellular calcium concentration ( $[Ca^{2+}]_i$ ) overload in dose- and time-dependent manners (Figure 5(A)).  $[Ca^{2+}]_i$  overload in the cytoplasm triggered the opening of the mitochondrial permeability transition pore, resulting in depolarization of mitochondrial membrane potential ( $\Delta\Psi$ ) (Figure 5(B)) and decrease in adenosine triphosphate (ATP) (Figure 5(C)) [22]. With the presence of insufficient cellular ATP, AMP-activated protein kinase (AMPK) was activated, leading to cell death [23].

Diosgenin and its derivatives are effective cytotoxic agents and induce apoptosis and autophagy in various types of cancer cells [17–19,24]. Poly ADP-ribose polymerase (PARP)

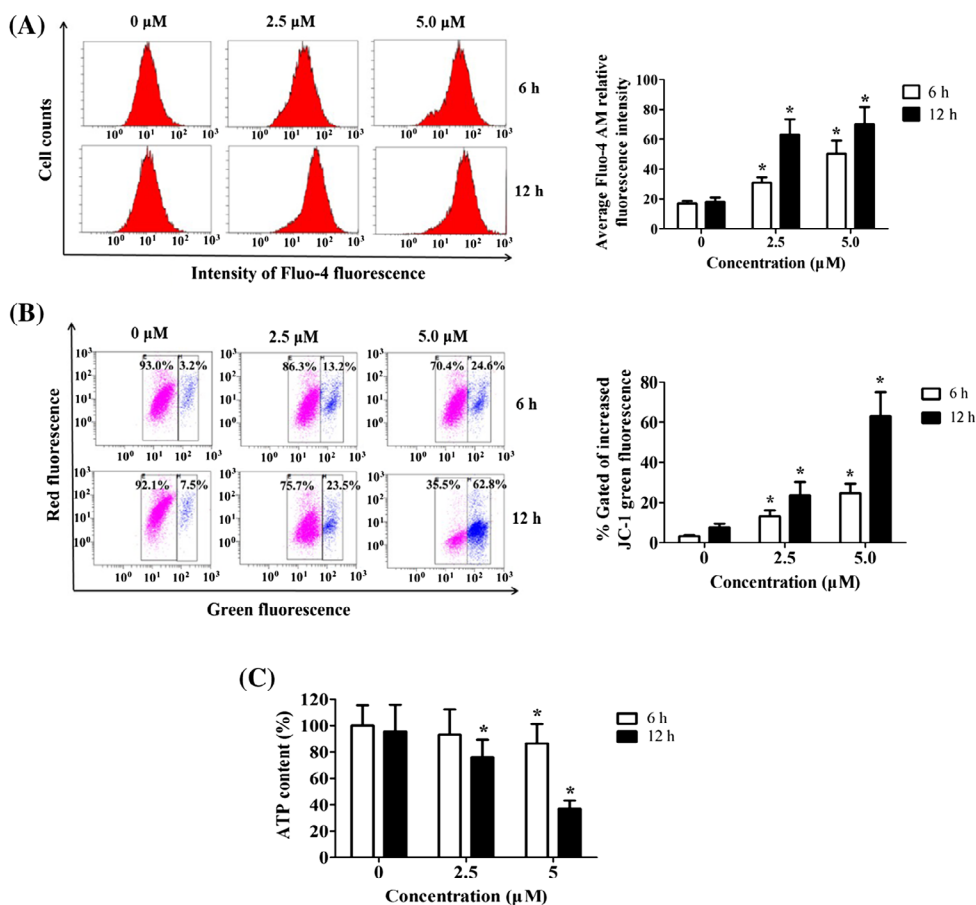


**Figure 5.** Influence of compound 4 on cellular calcium concentration, mitochondrial membrane potential and cellular ATP level in C26 cells. (A) Compound 4 increased cellular calcium concentration in C26 cells in dose- and time-dependent manners. (B) Compound 4 decreased mitochondrial membrane potential in C26 cells in dose- and time-dependent manners. (C) Compound 4 decreased cellular ATP level in C26 cells in dose- and time-dependent manners.

Note: \* $p < 0.05$  compared to control, error bars depict s.e.m.

is a nuclear enzyme that is involved in DNA repair. During apoptosis, PARP is specifically cleaved and inactivated by caspases. Accordingly, cleavage of PARP is a well-established marker for the detection of apoptosis. In the present study, PARP was found to be cleaved in C26 cells after 24 h of treatment with compound 4, implying activation of caspases that triggered apoptosis (Figure 6(A)). Morphological changes of C26 cells treated with compound 4 were characterized by TEM. It can be noted that compound 4 led to an increase in the number of autophagosomes (Figure 6(B)). The increase in endogenous PE-conjugated LC3-II after treatment with compound 4 further confirmed the activation of the autophagic response induced by compound 4 (Figure 6(C)). These results indicated that compound 4 inhibited tumor growth via apoptosis and autophagy. Consistently, diosgenin, one of diosgenyl saponins, also induced autophagy and apoptosis in human lung cancer cell lines [24].

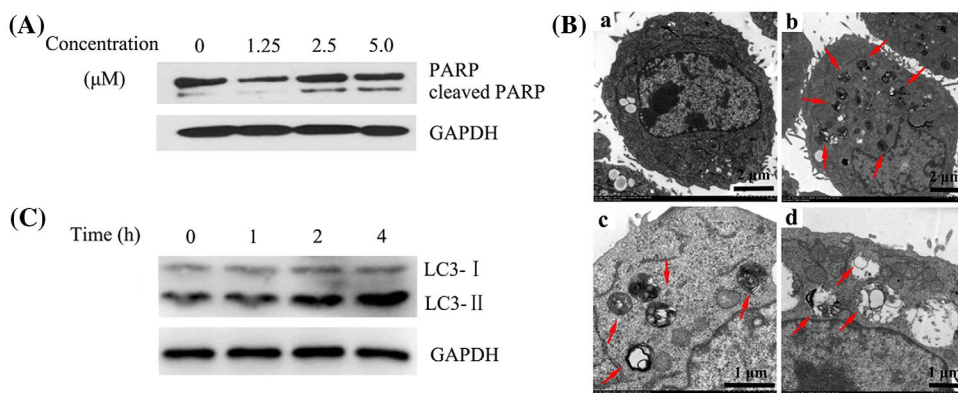


**Figure 6.** Compound 4 induced C26 cells death via apoptosis and autophagy. (A) C26 cells were treated with compound 4 (0, 1.25, 2.5 and 5 μM) for 24 h, and compound 4 induced cleavage of PARP in C26 cells to trigger cell apoptosis. (B) C26 cells were treated with compound 4 (0, 5 μM) for 24 h, and compound 4 increased autophagosome in cells and induced cells autophagy. a, The normal morphology of C26 cells by transmission electron micrograph; b, the changed morphology of C26 cells with autophagic vesicles after 24 h treatment with compound 4 (5 μM); c and d, the representatively enlarged images of C26 cells with typical autophagosomes and early autolysosomes (c) and late autolysosomes (d). (C) C26 cells were treated with compound 4 (5 μM) for different time, and compound 4 promoted the conversion of LC3-I to LC3-II.

To well evaluate the therapeutic potential of compound 4 on cancer *in vivo*, a tumor xenograft model of C26 cells was successfully established in this study [19]. As shown in Figure 7(A), the intraperitoneal administration of compound 4 at doses of 15 and 30 mg/kg results in the reduction of tumor growth by 26 and 44%, respectively, compared with control mice. During the experiment, no significant changes in the appetite, behavior, and weight of the mice were observed (Figure 7(B)). Furthermore, no significant pathological changes in the heart, liver, lung or kidney were detected by H&E staining (Figure 7(C)). Our previous study indicated that diosgenyl analogs could inhibit tumor growth through suppressing angiogenesis [18,19]. To further test whether compound 4 contributed to the inhibition of angiogenesis in tumor, we used immunohistochemical staining assay by anti-CD31 antibody to detect the microvessels in tumor tissues. It was noted that compound 4 significantly decreased the vessel density (Figure 7(D)). Our data showed that compound 4 significantly blocked C26 derived-tumor growth by suppressing angiogenesis without obvious toxicity *in vivo*. In summary, compound 4 is a potential anticancer drug candidate.

## 2.5. Structure–activity relationship of diosgenyl analogs on thrombosis

The preliminary antithrombotic activity of the diosgenyl analogs was evaluated using a mice tail bleeding time assay [11]. Diosgenin (1) and the representative diosgenyl analogs (4, 16 and 22) with 6-carbon atom side chains were selected for testing. To investigate the effect of these analogs on thrombosis, we measured tail bleeding times 1 h after the last administration. As shown in Figure 8, the bleeding times of the control group and diosgenin group were 342 and 532 s, respectively. Compounds 4 and 22, which had spiroketal structures (S-A), exhibited excellent efficacy in prolonging

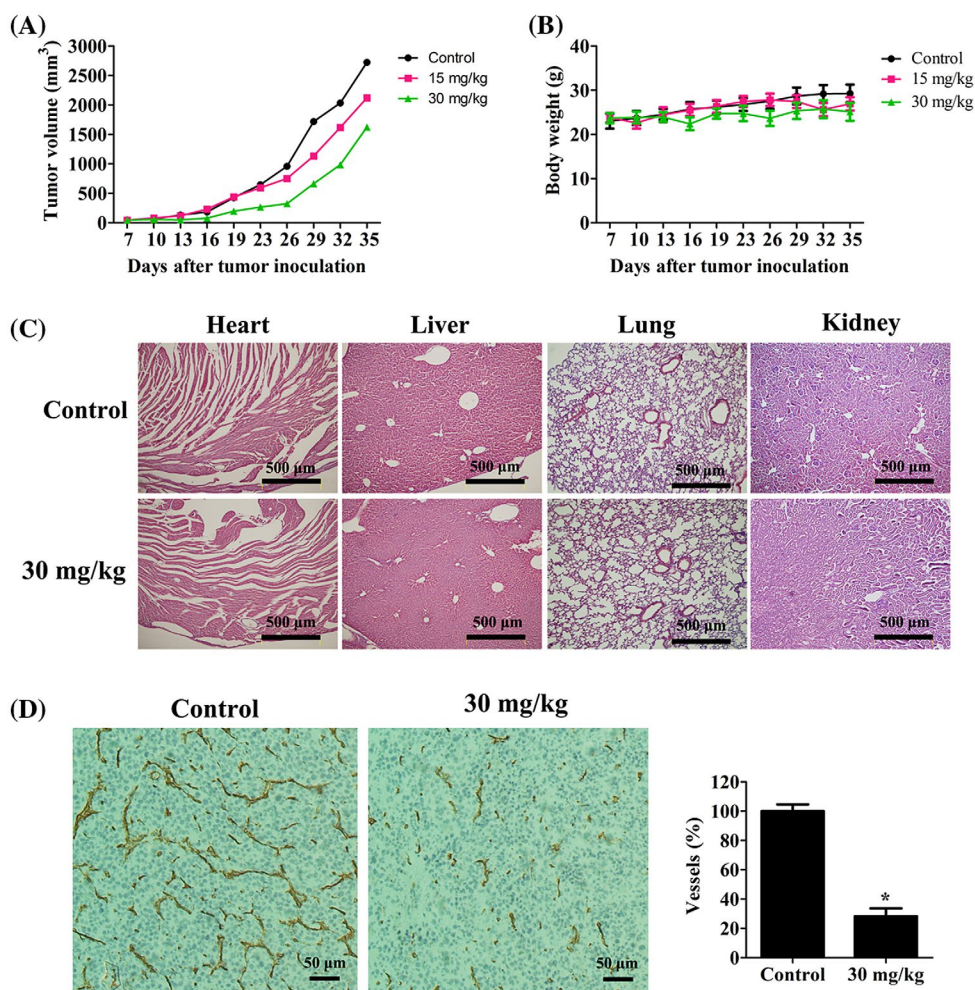


**Figure 7.** Compound 4 inhibited tumor growth and angiogenesis in C26 implanted-tumor mouse model *in vivo*. (A) Compound 4 suppressed tumor growth in C26 tumor models. (B) Toxicity-dependent weight loss in tumor-bearing mice treated with compound 4. There are no significant differences in weight between the three groups. (C) Typical H&E staining of paraffin embedded sections of the heart, liver, lung and kidney. Compound 4 did not cause obvious pathologic abnormalities in normal tissues. (D) Frozen sections of tumor tissues were tested by immune histochemical analysis with anti-CD31 antibody. Compound 4 blocked blood vessel growth within tumors.

Note: \* $p < 0.05$  compared to control, error bars depict s.e.m.

bleeding time. Unexpectedly, compound 16, which had furostanic structure (S-C), exhibited the opposite effect and reduced bleeding time compared to that observed for the control group and the diosgenin group. Our data indicated that diosgenyl analogs with spiroketal structures (S-A) blocked thrombosis while diosgenyl analogs with furostanic structures (S-C) promoted thrombosis.

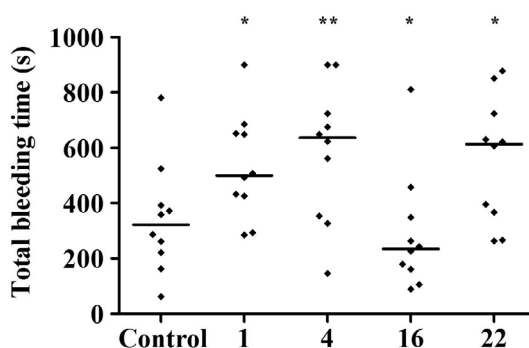


**Figure 8.** Effect of diosgenyl analogues 1, 4, 16 and 22 on tail bleeding time in mice.

Notes: The saline was used as the control,  $n = 10$  per group. Total bleeding times were recorded within 15 min. Horizontal bars represent means. \* $p < 0.05$  and \*\* $p < 0.01$  compared with control.

### 3. Conclusion

As an extension of our previous study, we synthesized 12 straight-chain amino acid diosgenyl analogs, five straight-chain fatty acid diosgenyl derivatives, and two fluorescence-labeled diosgenyl conjugates with different aglycon skeleton structures (S-A, S-B, S-C) with diosgenin as the starting material to further evaluate the anticancer activity and antithrombotic properties of these compounds. Compound 4, which contained a spiroketal structure with a 6-aminohexanoic acid residue, was the most effective molecule in blocking cancer cell growth *in vitro* and *in vivo*. It rapidly accumulates in the cytoplasm (but not in the nucleus), induces the accumulation of intracellular  $\text{Ca}^{2+}$ , induces loss of  $\Delta\Psi_m$  and decrease of cellular ATP, arrests the cell cycle in S-phase, and induces cell apoptosis and autophagy. Structure–activity relationship studies indicated that spiroketal analogs exhibited higher antithrombotic activity than diosgenin, and that furostanic analogs exhibited the opposite effect of spiroketal analogs by promoting thrombosis. Our study also indicated that the aglycon structure and the length of the carbon chain of straight-chain amino acid residues in diosgenyl analogs were both important for the antitumor and antithrombotic activity of the analogs.

Compound 4 effectively blocks tumor growth and inhibits thrombosis, suggesting that it may be a promising anticancer drug candidate and may have translational potential to complement currently used clinical drugs for cancer patients with thromboembolism. Further investigation of the biological behavior of diosgenyl analogs is needed to elucidate their anticancer effects and antithrombotic properties.

## 4. Experimental

### 4.1. Materials and methods

All air and moisture sensitive reactions were performed under nitrogen atmosphere. Anhydrous pyridine was distilled over potassium hydroxide, dry dichloromethane over calcium hydride. Unless otherwise stated, all commercially available reagents and solvents were used as supplied without further purification. The structural characterization of compounds was performed by NMR and high-resolution mass spectrometry.  $^1\text{H}$  NMR and  $^{13}\text{C}$

NMR spectra were recorded on Varian UNITY INOVA 400 or Bruker AV II-600 spectrometer with tetramethylsilane as an internal standard, and chemical shifts are reported in  $\delta$  (ppm). HRESIMS were obtained with ESI-Q-TOF-MS (Bruker Daltonics, Billerica, USA). Analytical thin-layer chromatography (TLC) was performed on Merck 60 F<sub>254</sub> silica gel plates, and visualization performed by UV or by spraying with sulfuric acid or ninhydrin. Column chromatography was performed with silica gel H 60 (200–300 mesh, Qingdao, China).

## 4.2. Chemical synthesis

### 4.2.1. Synthesis of (22 $\beta$ , 25R)-spirost-5-en-3 $\beta$ -yl amino acid esters (2–6)

**4.2.1.1. General procedure for the synthesis of tert-butoxycarbonyl amino acid esters 3b–6b.** Di-tert-butyl dicarbonate ((Boc)<sub>2</sub>O, 11.0 mmol) in a solution of CH<sub>3</sub>COCH<sub>3</sub> (5 ml) was added dropwise to a stirred solution of amino acid (**3a–6a**, 10.0 mmol) and triethylamine (Et<sub>3</sub>N, 20.0 mmol) in acetone-water (v:v 1:1, 20 ml), and the resulting solution was stirred for 4–8 h at room temperature until absence of amino acid (checked by TLC). The organic component of the solvent was removed under vacuum and the aqueous residue was acidified with dilute HCl until pH 4–5. The solution was extracted with EtOAc, and the combined organic fractions were washed with brine, dried over anhydrous Na<sub>2</sub>SO<sub>4</sub>, and then concentrated *in vacuo* and freeze-dried in –80 °C to yield **3b–6b**.

*N*-tert-Butoxycarbonyl-4-aminobutyric acid (**3b**): light yellow solid, (94%);  $R_f$  = 0.59 (CH<sub>2</sub>Cl<sub>2</sub>/CH<sub>3</sub>OH/CH<sub>3</sub>COOH 9:1:0.1); <sup>1</sup>H NMR (400 MHz, CDCl<sub>3</sub>)  $\delta$  11.19 (s, 1H), 4.76 (s, 1H), 3.19 (d,  $J$  = 5.7 Hz, 2H), 2.39 (t,  $J$  = 7.2 Hz, 2H), 1.93–1.72 (m, 2H), 1.44 (s, 9H); <sup>13</sup>C NMR (100 MHz, CDCl<sub>3</sub>)  $\delta$  177.4, 155.2, 78.5, 38.8, 30.3, 27.4, 24.1; HRESIMS:  $m/z$  204.1226 [M + H]<sup>+</sup> (calcd for C<sub>9</sub>H<sub>18</sub>NO<sub>4</sub>, 204.1236).

*N*-tert-Butoxycarbonyl-8-aminooctanoic acid (**5b**): light yellow solid, (93%);  $R_f$  = 0.58 (CH<sub>2</sub>Cl<sub>2</sub>/CH<sub>3</sub>OH/CH<sub>3</sub>COOH 9:1:0.1); <sup>1</sup>H NMR (400 MHz, CDCl<sub>3</sub>)  $\delta$  10.99 (s, 1H), 4.51 (s, 1H), 3.03 (d,  $J$  = 5.9 Hz, 2H), 2.26 (t,  $J$  = 7.5 Hz, 2H), 1.63–1.49 (m, 2H), 1.37 (s, 11H), 1.25 (s, 6H); <sup>13</sup>C NMR (100 MHz, CDCl<sub>3</sub>)  $\delta$  178.3, 155.0, 78.1, 39.5, 33.0, 28.9, 27.9, 27.4, 25.5, 23.6; HRESIMS:  $m/z$  260.1808 [M + H]<sup>+</sup> (calcd for C<sub>13</sub>H<sub>26</sub>NO<sub>2</sub>, 260.1862).

*N*-tert-Butoxycarbonyl-12-aminolauric acid (**6b**): light yellow solid, (95%);  $R_f$  = 0.60 (CH<sub>2</sub>Cl<sub>2</sub>/CH<sub>3</sub>OH/CH<sub>3</sub>COOH 9:1:0.1); <sup>1</sup>H NMR (400 MHz, CDCl<sub>3</sub>)  $\delta$  11.39 (s, 1H), 4.50 (s, 1H), 3.03 (d,  $J$  = 5.8 Hz, 2H), 2.27 (t,  $J$  = 7.5 Hz, 2H), 1.65–1.47 (m, 2H), 1.37 (s, 11H), 1.20 (s, 14H); <sup>13</sup>C NMR (100 MHz, CDCl<sub>3</sub>)  $\delta$  178.4, 155.0, 78.1, 39.6, 33.1, 29.0, 28.4, 28.2, 28.0, 27.4, 25.8, 23.7; HRESIMS:  $m/z$  338.2229 [M + Na]<sup>+</sup> (calcd for C<sub>17</sub>H<sub>33</sub>NO<sub>4</sub>Na, 338.2307).

**4.2.1.2. General procedure for the synthesis of (22 $\beta$ , 25R)-spirost-5-en-3 $\beta$ -yl *N*-tert-butoxycarbonyl amino acid esters 2c–6c.** Compounds **2c** and **4c** were synthesized as per reported method [13].

To a solution of compound **1** (2.0 mmol), **2b–6b** (2.5 mmol), DMAP (0.4 mmol) in anhydrous CH<sub>2</sub>Cl<sub>2</sub> (20 ml), EDC·HCl (2.5 mmol) in CH<sub>2</sub>Cl<sub>2</sub> (6 ml) was added dropwise under N<sub>2</sub> atmosphere. The mixture was left to stir at room temperature for 4–16 h under a balloon of nitrogen (checked by TLC). Then the reaction solution was washed with brine, saturated NaHCO<sub>3</sub> solution and brine, dried over anhydrous Na<sub>2</sub>SO<sub>4</sub>, and then filtered and concentrated. The residue was purified by a silica gel column chromatography (petroleum ether/EtOAc 12:1–8:1) to give **2c–6c**.

(22 $\beta$ , 25R)-Spirost-5-en-3 $\beta$ -yl *N*-tert-butoxycarbonyl-4-aminobutyrate (**3c**): white solid (81%);  $R_f$  = 0.30 (petroleum ether/EtOAc 4:1);  $^1\text{H}$  NMR (400 MHz,  $\text{CDCl}_3$ )  $\delta$  5.30 (d,  $J$  = 4.9 Hz, 1H), 4.64–4.41 (m, 2H), 4.34 (dd,  $J$  = 15.0, 7.5 Hz, 1H), 3.44–3.35 (m, 1H), 3.30 (t,  $J$  = 10.9 Hz, 1H), 3.09 (d,  $J$  = 5.8 Hz, 2H), 2.38–2.13 (m, 4H), 2.01–1.85 (m, 2H), 0.97 (s, 3H), 0.90 (d,  $J$  = 6.9 Hz, 3H), 0.72 (t,  $J$  = 3.1 Hz, 6H);  $^{13}\text{C}$  NMR (100 MHz,  $\text{CDCl}_3$ )  $\delta$  171.7, 154.9, 138.6, 121.4, 108.3, 79.8, 73.0, 65.8, 61.1, 55.4, 48.9, 40.6, 39.2, 38.7, 37.1, 35.9, 35.7, 31.0, 30.8, 30.4, 29.3, 27.8, 27.4, 26.7, 24.3, 19.8, 18.3, 16.1, 15.3, 13.5; HRESIMS:  $m/z$  600.4294  $[\text{M} + \text{H}]^+$  (calcd for  $\text{C}_{36}\text{H}_{58}\text{NO}_6$ , 600.4264).

(22 $\beta$ , 25R)-Spirost-5-en-3 $\beta$ -yl *N*-tert-butoxycarbonyl-8-aminooctanoate (**5c**): white solid (77%);  $R_f$  = 0.41 (petroleum ether/EtOAc 4:1);  $^1\text{H}$  NMR (400 MHz,  $\text{CDCl}_3$ )  $\delta$  5.30 (d,  $J$  = 5.0 Hz, 1H), 4.59–4.49 (m, 1H), 4.43 (s, 1H), 4.34 (dd,  $J$  = 14.9, 7.5 Hz, 1H), 3.45–3.35 (m, 1H), 3.30 (t,  $J$  = 10.9 Hz, 1H), 3.02 (t,  $J$  = 7.0 Hz, 2H), 2.31–2.13 (m, 4H), 1.98–1.86 (m, 2H), 1.84–1.74 (m, 3H), 0.97 (s, 3H), 0.90 (d,  $J$  = 6.9 Hz, 3H), 0.72 (t,  $J$  = 3.1 Hz, 6H);  $^{13}\text{C}$  NMR (100 MHz,  $\text{CDCl}_3$ )  $\delta$  172.2, 155.0, 138.7, 121.3, 108.2, 79.8, 72.6, 65.8, 61.1, 55.4, 48.9, 40.6, 39.2, 38.7, 37.1, 36.0, 35.7, 33.6, 31.0, 30.8, 30.4, 29.3, 29.0, 28.0, 27.9, 27.8, 27.4, 26.8, 25.6, 23.9, 19.8, 18.3, 16.1, 15.3, 13.5; HRESIMS:  $m/z$  656.4808  $[\text{M} + \text{H}]^+$  (calcd for  $\text{C}_{40}\text{H}_{66}\text{NO}_6$ , 656.4890).

(22 $\beta$ , 25R)-Spirost-5-en-3 $\beta$ -yl *N*-tert-butoxycarbonyl-12-aminolaurate (**6c**): white solid (82%);  $R_f$  = 0.48 (petroleum ether/EtOAc 4:1);  $^1\text{H}$  NMR (400 MHz,  $\text{CDCl}_3$ )  $\delta$  5.30 (d,  $J$  = 4.9 Hz, 1H), 4.65–4.48 (m, 1H), 4.42 (s, 1H), 4.34 (dd,  $J$  = 15.0, 7.5 Hz, 1H), 3.40 (dd,  $J$  = 10.1, 3.4 Hz, 1H), 3.30 (t,  $J$  = 10.9 Hz, 1H), 3.02 (t,  $J$  = 7.1 Hz, 2H), 2.28–2.14 (m, 4H), 1.98–1.86 (m, 2H), 1.83–1.74 (m, 3H), 0.97 (s, 3H), 0.90 (d,  $J$  = 6.9 Hz, 3H), 0.72 (t,  $J$  = 3.1 Hz, 6H);  $^{13}\text{C}$  NMR (100 MHz,  $\text{CDCl}_3$ )  $\delta$  172.3, 155.0, 138.8, 121.3, 108.2, 79.8, 72.6, 65.8, 61.1, 55.4, 48.9, 40.6, 39.2, 38.7, 37.1, 36.0, 35.7, 33.7, 31.0, 30.8, 30.4, 29.3, 29.1, 28.5, 28.4, 28.3, 28.2, 28.1, 27.8, 27.4, 26.8, 25.8, 24.0, 19.8, 18.3, 16.1, 15.3, 13.5; HRESIMS:  $m/z$  712.5445  $[\text{M} + \text{H}]^+$  (calcd for  $\text{C}_{44}\text{H}_{74}\text{NO}_6$ , 712.5516).

**4.2.1.3. General procedure for the synthesis of (22 $\beta$ , 25R)-spirost-5-en-3 $\beta$ -yl amino acid esters 2–6.**  $\text{CF}_3\text{COOH}$  (20.0 mmol) was added to a stirred solution of **2c–6c** (1.5 mmol) in  $\text{CH}_2\text{Cl}_2$  (20 ml) at room temperature for 4–10 h. Then the mixture solution was removed *in vacuo* and purified by column chromatography ( $\text{CH}_2\text{Cl}_2/\text{CH}_3\text{COCH}_3$  5:1–2:1) to yield compounds 2–6.

Compounds **2** and **4** were synthesized as per reported method [13].

(22 $\beta$ , 25R)-Spirost-5-en-3 $\beta$ -yl 4-aminobutyrate (**3**): light yellow solid, (87%);  $R_f$  = 0.19 ( $\text{CH}_2\text{Cl}_2/\text{CH}_3\text{OH}/\text{CH}_3\text{COOH}$  6:1:0.1);  $^1\text{H}$  NMR (400 MHz,  $\text{CDCl}_3$ )  $\delta$  5.37 (d,  $J$  = 4.6 Hz, 1H), 4.67–4.53 (m, 1H), 4.41 (dd,  $J$  = 15.0, 7.4 Hz, 1H), 3.51–3.32 (m, 4H), 2.79 (t,  $J$  = 6.9 Hz, 2H), 2.38–2.28 (m, 4H), 2.05–1.92 (m, 2H), 1.03 (s, 3H), 0.97 (d,  $J$  = 6.9 Hz, 3H), 0.79 (t,  $J$  = 3.1 Hz, 6H);  $^{13}\text{C}$  NMR (100 MHz,  $\text{CDCl}_3$ )  $\delta$  171.1, 138.6, 121.4, 108.2, 79.8, 73.4, 65.8, 61.1, 55.5, 48.9, 40.6, 39.7, 39.2, 38.7, 38.4, 37.0, 35.9, 35.7, 31.0, 30.8, 30.5, 30.4, 29.3, 27.8, 26.7, 21.7, 19.8, 18.3, 16.1, 15.3, 13.5; HRESIMS:  $m/z$  500.3780  $[\text{M} + \text{H}]^+$  (calcd for  $\text{C}_{31}\text{H}_{50}\text{NO}_4$ , 500.3740).

(22 $\beta$ , 25R)-Spirost-5-en-3 $\beta$ -yl 8-aminooctanoate (**5**): light yellow solid, (84%);  $R_f$  = 0.31 ( $\text{CH}_2\text{Cl}_2/\text{CH}_3\text{OH}/\text{CH}_3\text{COOH}$  6:1:0.1);  $^1\text{H}$  NMR (400 MHz,  $\text{CDCl}_3$ )  $\delta$  5.37 (d,  $J$  = 4.7 Hz, 1H), 4.68–4.54 (m, 1H), 4.41 (dd,  $J$  = 15.0, 7.5 Hz, 1H), 3.47 (dd,  $J$  = 10.2, 3.3 Hz, 1H), 3.37 (t,  $J$  = 10.9 Hz, 1H), 2.68 (t,  $J$  = 7.0 Hz, 2H), 2.35–2.20 (m, 4H), 1.04 (s, 3H), 0.97 (d,  $J$  = 6.9 Hz, 3H), 0.79 (t,  $J$  = 3.0 Hz, 6H);  $^{13}\text{C}$  NMR (100 MHz,  $\text{CDCl}_3$ )  $\delta$  172.2, 138.7, 121.3,

108.3, 79.8, 72.7, 65.8, 61.1, 55.4, 48.9, 44.9, 40.6, 39.2, 38.9, 38.7, 37.1, 36.0, 35.7, 33.5, 31.0, 30.8, 30.4, 29.3, 27.8, 27.6, 26.8, 26.5, 25.3, 23.8, 19.8, 18.3, 16.1, 15.3, 13.5, 7.7; HRESIMS:  $m/z$  556.4348  $[M + H]^+$  (calcd for  $C_{35}H_{58}NO_4$ , 556.4366).

(22 $\beta$ , 25R)-Spirost-5-en-3 $\beta$ -yl 12-aminolaurate (**6**): light yellow solid, (80%);  $R_f$  = 0.42 ( $CH_2Cl_2/CH_3OH/CH_3COOH$  6:1:0.1);  $^1H$  NMR (400 MHz,  $CDCl_3$ )  $\delta$  5.37 (d,  $J$  = 4.9 Hz, 1H), 4.67–4.53 (m, 1H), 4.41 (dd,  $J$  = 15.0, 7.5 Hz, 1H), 3.51–3.44 (m, 1H), 3.37 (t,  $J$  = 10.9 Hz, 1H), 2.72 (t,  $J$  = 7.2 Hz, 2H), 2.34–2.23 (m, 4H), 2.04–1.93 (m, 2H), 1.90–1.81 (m, 3H), 1.04 (s, 3H), 0.97 (d,  $J$  = 6.9 Hz, 3H), 0.79 (t,  $J$  = 3.1 Hz, 6H);  $^{13}C$  NMR (100 MHz,  $CDCl_3$ )  $\delta$  173.3, 139.8, 122.3, 109.3, 80.8, 73.6, 66.8, 62.1, 56.4, 49.9, 41.6, 40.3, 39.7, 38.1, 37.0, 36.7, 34.7, 32.0, 31.8, 31.4, 30.3, 29.5, 29.4, 29.3, 29.1, 28.8, 27.8, 26.8, 25.1, 20.8, 19.3, 17.1, 16.3, 14.5; HRESIMS:  $m/z$  612.4990  $[M + H]^+$  (calcd for  $C_{39}H_{66}NO_4$ , 612.4992).

#### 4.2.2. Synthesis of (25R)-furost-5-en-26-ol-3 $\beta$ -yl amino acid esters (7–11)

**4.2.2.1. General procedure for the synthesis of (25R)-furost-5-en-26-ol-3 $\beta$ -yl *N*-tert-butoxycarbonyl amino acid esters 7a–11a.** Compounds **2c–6c** were stirred with  $CH_3COOH$  (12 ml) in  $CH_2Cl_2$  (6 ml) at room temperature for 30 min, and then sodium cyanoborohydride (8 mmol) was added in portions over a period of 45 min. This mixture was left to stir at room temperature overnight. Then brine (10 ml) was added and extracted with  $CH_2Cl_2$  (15 ml\*3). The solution was washed with brine, saturated  $NaHCO_3$  solution and brine, respectively. After drying the organic layer with  $Na_2SO_4$  and filtering, the solvent was removed *in vacuo* and purified by column chromatography (petroleum ether/EtOAc 5:1–3:1) to yield **7a–11a**.

(25R)-Furost-5-en-26-ol-3 $\beta$ -yl *N*-tert-butoxycarbonyl-glycinate (**7a**): white solid (82%);  $R_f$  = 0.44 (petroleum ether/EtOAc 1:1);  $^1H$  NMR (400 MHz,  $CDCl_3$ )  $\delta$  5.37 (d,  $J$  = 4.3 Hz, 1H), 5.06 (s, 1H), 4.73–4.61 (m, 1H), 4.35–4.26 (m, 1H), 3.87 (s, 2H), 3.49 (dd,  $J$  = 10.6, 6.2 Hz, 1H), 3.43 (dd,  $J$  = 10.6, 6.2 Hz, 1H), 3.37–3.29 (m, 1H), 2.33 (d,  $J$  = 7.8 Hz, 2H), 2.06–1.93 (m, 3H), 1.87 (d,  $J$  = 10.4 Hz, 2H), 1.45 (s, 10H), 1.03 (s, 3H), 1.00 (d,  $J$  = 6.7 Hz, 3H), 0.91 (d,  $J$  = 6.7 Hz, 3H), 0.81 (s, 3H);  $^{13}C$  NMR (100 MHz,  $CDCl_3$ )  $\delta$  168.7, 154.7, 138.4, 121.6, 89.3, 82.2, 78.9, 74.0, 67.0, 64.1, 55.9, 49.0, 41.6, 39.7, 38.4, 37.0, 36.9, 35.9, 35.7, 34.7, 31.2, 31.0, 30.5, 29.5, 29.1, 28.7, 27.3, 26.7, 19.6, 18.3, 17.9, 15.6, 15.4; HRESIMS:  $m/z$  596.3937  $[M + Na]^+$  (calcd for  $C_{34}H_{55}NO_6Na$ , 596.3927).

(25R)-Furost-5-en-26-ol-3 $\beta$ -yl *N*-tert-butoxycarbonyl-4-aminobutyrate (**8a**): white solid (85%);  $R_f$  = 0.41 (petroleum ether/EtOAc 1:1);  $^1H$  NMR (400 MHz,  $CDCl_3$ )  $\delta$  5.37 (d,  $J$  = 4.8 Hz, 1H), 4.71–4.54 (m, 2H), 4.34–4.27 (m, 1H), 3.50 (dd,  $J$  = 10.6, 6.2 Hz, 1H), 3.43 (dd,  $J$  = 10.6, 6.2 Hz, 1H), 3.33 (m, 1H), 3.16 (t,  $J$  = 6.8 Hz, 2H), 2.32 (t,  $J$  = 7.3 Hz, 4H), 2.09–1.91 (m, 3H), 1.44 (s, 9H), 1.03 (s, 3H), 1.00 (d,  $J$  = 6.7 Hz, 3H), 0.91 (d,  $J$  = 6.7 Hz, 3H), 0.81 (s, 3H);  $^{13}C$  NMR (100 MHz,  $CDCl_3$ )  $\delta$  171.7, 154.9, 138.6, 121.4, 89.3, 82.2, 78.3, 73.0, 67.0, 64.1, 55.9, 49.0, 39.7, 38.4, 37.1, 36.9, 36.0, 35.7, 34.7, 31.2, 31.0, 30.5, 29.5, 29.2, 27.4, 26.7, 24.3, 19.6, 18.3, 17.9, 15.6, 15.4; HRESIMS:  $m/z$  624.4233  $[M + Na]^+$  (calcd for  $C_{36}H_{59}NO_6Na$ , 624.4240).

(25R)-Furost-5-en-26-ol-3 $\beta$ -yl *N*-tert-butoxycarbonyl-12-aminolaurate (**11a**): white solid (80%);  $R_f$  = 0.56 (petroleum ether/EtOAc 1:1);  $^1H$  NMR (400 MHz,  $CDCl_3$ )  $\delta$  5.37 (d,  $J$  = 4.8 Hz, 1H), 4.65–4.56 (m, 1H), 4.52 (s, 1H), 4.34–4.26 (m, 1H), 3.50 (dd,  $J$  = 10.6, 6.2 Hz, 1H), 3.43 (dd,  $J$  = 10.6, 6.2 Hz, 1H), 3.37–3.28 (m, 1H), 3.09 (t,  $J$  = 7.1 Hz, 2H), 2.35–2.21 (m, 4H), 2.06–1.94 (m, 3H), 1.89–1.81 (m, 2H), 1.44 (s, 9H), 1.04 (s, 3H), 1.00 (d,  $J$  = 6.7 Hz, 3H), 0.91 (d,  $J$  = 6.7 Hz, 3H), 0.81 (s, 3H);  $^{13}C$  NMR (100 MHz,  $CDCl_3$ )  $\delta$  172.3, 155.0, 138.7,

121.3, 89.4, 82.2, 78.0, 72.6, 67.0, 64.1, 55.9, 49.0, 39.7, 38.4, 37.1, 36.9, 36.0, 35.7, 34.7, 33.7, 31.2, 31.0, 30.6, 29.5, 29.2, 29.1, 28.5, 28.4, 28.3, 28.2, 28.1, 27.4, 26.8, 25.8, 24.0, 19.6, 18.3, 17.9, 15.6, 15.4; HRESIMS:  $m/z$  736.5493  $[M + Na]^+$  (calcd for  $C_{44}H_{75}NO_6Na$ , 736.5492).

**4.2.2.2. General procedure for the synthesis of (25R)-furost-5-en-26-ol-3 $\beta$ -yl amino acid esters 7–11.**  $CF_3COOH$  (20.0–30.0 mmol) was added to a stirred solution of **7a–11a** (1.0–1.5 mmol) in  $CH_2Cl_2$  (20 ml) at 30–35 °C and kept for 2–6 h. Then the mixture solution was removed in vacuo to give the crude product which was purified by column chromatography ( $CH_2Cl_2/CH_3OH$  15:1) to yield compounds **7–11**.

(25R)-Furost-5-en-26-ol-3 $\beta$ -yl glycinate (**7**): white solid (78%);  $R_f$  = 0.38 ( $CH_2Cl_2/CH_3OH/CH_3COOH$  6:1:0.1);  $^1H$  NMR (400 MHz,  $CDCl_3$ )  $\delta$  5.37 (s, 1H), 4.73–4.55 (m, 1H), 4.30 (dd,  $J$  = 13.2, 7.3 Hz, 1H), 4.27–4.11 (m, 1H), 3.77 (s, 2H), 3.53–3.41 (m, 1H), 3.38–3.26 (m, 1H), 2.33 (d,  $J$  = 24.1 Hz, 2H), 0.81 (s, 3H);  $^{13}C$  NMR (100 MHz,  $CDCl_3$ )  $\delta$  167.0, 139.1, 122.8, 90.0, 83.2, 72.7, 68.0, 65.2, 57.0, 50.0, 40.7, 39.5, 37.9, 37.6, 36.9, 36.6, 35.7, 32.6, 32.0, 31.5, 30.6, 30.1, 27.3, 20.7, 19.3, 18.9, 16.6, 16.4; HRESIMS:  $m/z$  474.3563  $[M + H]^+$  (calcd for  $C_{29}H_{48}NO_4$ , 474.3583).

(25R)-Furost-5-en-26-ol-3 $\beta$ -yl 4-aminobutyrate (**8**): light yellow solid (82%);  $R_f$  = 0.32 ( $CH_2Cl_2/CH_3OH/CH_3COOH$  6:1:0.1);  $^1H$  NMR (400 MHz,  $CDCl_3$ )  $\delta$  5.36 (d,  $J$  = 3.7 Hz, 1H), 4.65–4.51 (m, 1H), 4.31 (dd,  $J$  = 13.2, 7.5 Hz, 1H), 4.25 (dd,  $J$  = 10.6, 5.7 Hz, 1H), 4.16 (dd,  $J$  = 10.6, 6.9 Hz, 1H), 3.53–3.41 (m, 1H), 3.39–3.26 (m, 1H), 3.02 (s, 2H), 2.42 (t,  $J$  = 6.7 Hz, 2H), 2.30 (d,  $J$  = 7.8 Hz, 2H), 1.05–0.96 (m, 9H), 0.80 (s, 3H);  $^{13}C$  NMR (100 MHz,  $CDCl_3$ )  $\delta$  172.7, 139.5, 122.5, 89.9, 83.3, 74.9, 72.7, 65.1, 56.9, 50.0, 40.7, 39.5, 39.4, 37.9, 36.9, 36.7, 32.6, 32.2, 32.0, 31.6, 31.4, 30.6, 30.1, 27.5, 22.3, 20.7, 19.3, 18.9, 16.4; HRESIMS:  $m/z$  502.3893  $[M + H]^+$  (calcd for  $C_{31}H_{52}NO_4$ , 502.3896).

(25R)-Furost-5-en-26-ol-3 $\beta$ -yl 12-aminolaurate (**11**): light yellow viscous solid (75%);  $R_f$  = 0.31 ( $CH_2Cl_2/CH_3OH/CH_3COOH$  6:1:0.1);  $^1H$  NMR (400 MHz, MeOD)  $\delta$  5.29 (d,  $J$  = 4.7 Hz, 1H), 4.50–4.37 (m, 1H), 4.27–4.17 (m, 1H), 3.32 (dd,  $J$  = 10.7, 5.9 Hz, 1H), 3.23–3.18 (m, 2H), 2.81 (m, 2H), 2.19 (dd,  $J$  = 15.7, 8.2 Hz, 4H), 1.97–1.86 (m, 2H), 1.81 (m, 1H), 1.77–1.63 (m, 3H), 0.97 (s, 3H), 0.92 (d,  $J$  = 6.7 Hz, 3H), 0.81 (d,  $J$  = 6.7 Hz, 3H), 0.74 (s, 3H);  $^{13}C$  NMR (100 MHz, MeOD)  $\delta$  175.1, 141.1, 123.4, 91.7, 84.6, 75.2, 68.4, 66.6, 58.2, 51.6, 41.9, 40.8, 40.5, 39.3, 39.2, 38.3, 37.9, 37.0, 35.4, 33.2, 33.1, 32.9, 32.0, 31.2, 30.6, 30.5, 30.4, 30.2, 30.1, 28.9, 28.6, 27.5, 26.1, 21.8, 19.8, 19.3, 17.0; HRESIMS:  $m/z$  614.5142  $[M + H]^+$  (calcd for  $C_{39}H_{68}NO_4$ , 614.5148).

#### 4.2.3. Synthesis of (25R)-furost-5-en-3 $\beta$ -acetoxy-26-yl amino acid esters (14–17)

**4.2.3.1. Synthesis of (25R)-furost-5-en-3 $\beta$ -acetoxy-26-ol (13).** Acetic anhydride (20 ml, 213 mmol) was added to a solution of diosgenin (8.29 g, 20 mmol) in pyridine (60 ml) at room temperature. The solution was stirred at 60 °C for 1 h and then poured into ice-cool water (2000 ml). The crude yellowish solid was filtered through the silica washing with brine, dil. HCl and brine, the crude product was precipitated with methanol to yield compound **12**.

(22 $\beta$ ,25R)-Spirost-5-en-3 $\beta$ -acetate (**12**): white needle solid (93%);  $R_f$  = 0.54 (petroleum ether/EtOAc 4:1);  $^1H$  NMR (400 MHz,  $CDCl_3$ )  $\delta$  5.37 (d,  $J$  = 4.5 Hz, 1H), 4.78–4.49 (m, 1H), 4.41 (dd,  $J$  = 14.9, 7.5 Hz, 1H), 3.47 (dd,  $J$  = 10.0, 3.2 Hz, 1H), 3.37 (t,  $J$  = 10.9 Hz, 1H), 2.48–2.23 (m, 2H), 2.03 (s, 3H), 1.03 (s, 3H), 0.97 (d,  $J$  = 6.9 Hz, 3H), 0.79 (d,  $J$  = 3.9 Hz, 6H);  $^{13}C$  NMR (100 MHz,  $CDCl_3$ )  $\delta$  169.5, 138.7, 121.4, 108.3, 79.8, 72.9, 65.8, 61.1, 55.4,

48.9, 40.6, 39.2, 38.7, 37.1, 35.9, 35.7, 31.0, 30.8, 30.4, 29.3, 27.8, 26.7, 20.4, 19.8, 18.3, 16.1, 15.3, 13.5.

Compound **12** (2.28 g, 5 mmol) was dissolved in a mixture solution of CH<sub>3</sub>COOH/CH<sub>2</sub>Cl<sub>2</sub> (30 ml : 15 ml) at room temperature, and then, sodium cyanoborohydride (942 mg, 15 mmol) was added in portions over a period of 30 min. This mixture was stirred for 4 h at room temperature (checked by TLC). Then, brine (10 ml) was added and extracted with CH<sub>2</sub>Cl<sub>2</sub> for three times. The organic layer was dried over anhydrous Na<sub>2</sub>SO<sub>4</sub> and concentrated *in vacuo*. The crude mass was purified through silica gel column (petroleum ether/EtOAc 3:1) to yield **13**.

Compound **13** was synthesized as previously reported method [7].

(25*R*)-Furost-5-en-3β-acetoxy-26-ol (**13**): white needle solid (85%);  $R_f = 0.51$  (petroleum ether/EtOAc 1:1); <sup>1</sup>H NMR (600 MHz, CDCl<sub>3</sub>) δ 5.37 (d,  $J = 4.9$  Hz, 1H), 4.60 (tt,  $J = 10.5, 5.1$  Hz, 1H), 4.31 (dd,  $J = 13.1, 7.7$  Hz, 1H), 3.49 (dd,  $J = 10.6, 6.2$  Hz, 1H), 3.43 (dd,  $J = 10.6, 6.2$  Hz, 1H), 3.33 (td,  $J = 8.3, 3.8$  Hz, 1H), 2.36–2.27 (m, 2H), 2.03 (s, 3H), 2.02–1.96 (m, 3H), 1.86 (d,  $J = 10.6$  Hz, 2H), 1.03 (s, 3H), 1.00 (d,  $J = 6.7$  Hz, 3H), 0.91 (d,  $J = 6.7$  Hz, 3H), 0.81 (s, 3H); <sup>13</sup>C NMR (150 MHz, CDCl<sub>3</sub>) δ 170.5, 139.7, 122.4, 90.4, 83.2, 73.9, 68.0, 65.1, 56.9, 50.0, 40.7, 39.4, 38.1, 37.9, 37.0, 36.7, 35.7, 32.2, 32.0, 31.6, 30.5, 30.1, 27.7, 21.4, 20.6, 19.3, 18.9, 16.6, 16.4; HRESIMS:  $m/z$  481.3283 [M + Na]<sup>+</sup> (calcd for C<sub>29</sub>H<sub>46</sub>O<sub>4</sub>Na, 481.3294).

**4.2.3.2. General procedure for the synthesis of (25*R*)-furost-5-en-3β-acetoxy-26-yl *N*-tert-butoxycarbonyl amino acid esters **14a–17a**.** To a solution of compound **13** (1.0 mmol), **2b–6b** (1.2 mmol), DMAP (0.2 mmol) in anhydrous CH<sub>2</sub>Cl<sub>2</sub> (15 ml), EDC·HCl (1.2 mmol) in CH<sub>2</sub>Cl<sub>2</sub> (5 ml) was added dropwise under N<sub>2</sub> atmosphere. The mixture was left to stir at room temperature for 4–16 h under a balloon of nitrogen (checked by TLC). The reaction solution was washed with brine, saturated NaHCO<sub>3</sub> solution and brine, dried over anhydrous Na<sub>2</sub>SO<sub>4</sub>, and then filtered and concentrated. The residue was purified by a silica gel column chromatography (petroleum ether/EtOAc 12:1–8:1) to give **14a–17a**.

(25*R*)-Furost-5-en-3β-acetoxy-26-yl *N*-tert-butoxycarbonyl-glycinate (**14a**): white viscous solid (87%);  $R_f = 0.51$  (petroleum ether/EtOAc 2:1); <sup>1</sup>H NMR (400 MHz, CDCl<sub>3</sub>) δ 5.30 (d,  $J = 4.8$  Hz, 1H), 4.97 (s, 1H), 4.60–4.46 (m, 1H), 4.29–4.16 (m, 1H), 3.98 (dd,  $J = 10.6, 5.8$  Hz, 1H), 3.91–3.78 (m, 3H), 3.29–3.17 (m, 1H), 2.25 (d,  $J = 6.7$  Hz, 2H), 1.96 (s, 3H), 1.38 (s, 9H), 0.97 (s, 3H), 0.93 (d,  $J = 6.7$  Hz, 3H), 0.87 (d,  $J = 6.7$  Hz, 3H), 0.73 (s, 3H); <sup>13</sup>C NMR (100 MHz, CDCl<sub>3</sub>) δ 169.5, 154.7, 138.7, 121.4, 89.1, 82.2, 78.9, 72.9, 69.1, 64.1, 55.9, 49.0, 41.4, 39.7, 38.4, 37.1, 36.9, 36.0, 35.7, 31.7, 31.2, 31.0, 30.6, 29.7, 29.3, 28.7, 27.3, 26.7, 20.4, 19.6, 18.3, 17.9, 15.7, 15.4; HRESIMS:  $m/z$  638.4039 [M + Na]<sup>+</sup> (calcd for C<sub>36</sub>H<sub>57</sub>NO<sub>7</sub>Na, 638.4033).

(25*R*)-Furost-5-en-3β-acetoxy-26-yl *N*-tert-butoxycarbonyl-4-aminobutyrate (**15a**): white viscous solid (84%);  $R_f = 0.46$  (petroleum ether/EtOAc 2:1); <sup>1</sup>H NMR (400 MHz, CDCl<sub>3</sub>) δ 5.37 (d,  $J = 4.8$  Hz, 1H), 4.75 (s, 1H), 4.65–4.53 (m, 1H), 4.35–4.25 (m, 1H), 3.97 (dd,  $J = 10.7, 5.9$  Hz, 1H), 3.87 (dd,  $J = 10.7, 6.8$  Hz, 1H), 3.35–3.26 (m, 1H), 3.16 (dd,  $J = 12.5, 6.2$  Hz, 2H), 2.40–2.29 (m, 4H), 2.03 (s, 3H), 1.44 (s, 9H), 1.04 (s, 3H), 1.00 (d,  $J = 6.7$  Hz, 3H), 0.93 (d,  $J = 6.7$  Hz, 3H), 0.81 (s, 3H); <sup>13</sup>C NMR (100 MHz, CDCl<sub>3</sub>) δ 173.3, 170.5, 155.9, 139.7, 122.4, 90.1, 83.2, 79.1, 73.9, 69.3, 65.1, 56.9, 50.0, 40.7, 40.0, 39.4, 38.1, 37.9, 37.0, 36.7, 32.7, 32.2, 32.0, 31.6, 30.7, 30.4, 29.7, 28.4, 27.7, 26.9, 25.3, 21.4, 20.6, 19.3, 18.9, 16.8, 16.4, 14.1; HRESIMS:  $m/z$  666.4344 [M + Na]<sup>+</sup> (calcd for C<sub>38</sub>H<sub>61</sub>NO<sub>7</sub>Na, 666.4346).

(25R)-Furost-5-en-3 $\beta$ -acetoxy-26-yl *N*-tert-butoxycarbonyl-6-aminohexanoate (**16a**): white viscous solid (79%);  $R_f = 0.47$  (petroleum ether/EtOAc 2:1);  $^1\text{H}$  NMR (400 MHz,  $\text{CDCl}_3$ )  $\delta$  5.30 (d,  $J = 4.8$  Hz, 1H), 4.64–4.46 (m, 2H), 4.27–4.18 (m, 1H), 3.90 (dd,  $J = 10.7$ , 5.8 Hz, 1H), 3.79 (dd,  $J = 10.7$ , 6.8 Hz, 1H), 3.28–3.19 (m, 1H), 3.04 (dd,  $J = 12.8$ , 6.4 Hz, 2H), 2.24 (t,  $J = 7.5$  Hz, 4H), 1.96 (s, 3H), 1.37 (s, 9H), 0.97 (s, 3H), 0.93 (d,  $J = 6.7$  Hz, 3H), 0.86 (d,  $J = 6.7$  Hz, 3H), 0.74 (s, 3H);  $^{13}\text{C}$  NMR (100 MHz,  $\text{CDCl}_3$ )  $\delta$  172.7, 169.5, 155.0, 138.7, 121.4, 89.1, 82.2, 77.9, 72.9, 68.1, 64.1, 55.9, 49.0, 39.7, 39.4, 38.4, 37.1, 36.9, 36.0, 35.7, 33.2, 31.8, 31.2, 31.0, 30.6, 29.8, 29.4, 28.8, 28.7, 27.4, 26.7, 25.3, 23.7, 20.4, 19.6, 18.3, 17.9, 15.8, 15.4; HRESIMS:  $m/z$  672.4265  $[\text{M} + \text{H}]^+$  (calcd for  $\text{C}_{40}\text{H}_{66}\text{NO}_6$ , 672.4839).

(25R)-Furost-5-en-3 $\beta$ -acetoxy-26-yl *N*-tert-butoxycarbonyl-12-aminolaurate (**17a**): white viscous solid (88%);  $R_f = 0.59$  (petroleum ether/EtOAc 2:1);  $^1\text{H}$  NMR (400 MHz,  $\text{CDCl}_3$ )  $\delta$  5.37 (d,  $J = 4.9$  Hz, 1H), 4.67–4.56 (m, 1H), 4.53 (s, 1H), 4.30 (td,  $J = 7.7$ , 5.4 Hz, 1H), 3.97 (dd,  $J = 10.7$ , 5.7 Hz, 1H), 3.86 (dd,  $J = 10.7$ , 6.8 Hz, 1H), 3.30 (td,  $J = 8.0$ , 4.3 Hz, 1H), 3.09 (s, 2H), 2.30 (dd,  $J = 14.9$ , 7.4 Hz, 4H), 1.04 (s, 3H), 1.00 (d,  $J = 6.7$  Hz, 3H), 0.93 (d,  $J = 6.7$  Hz, 3H), 0.81 (s, 3H);  $^{13}\text{C}$  NMR (100 MHz,  $\text{CDCl}_3$ )  $\delta$  174.0, 170.5, 156.0, 139.7, 122.4, 90.2, 83.2, 79.0, 73.9, 69.1, 65.1, 56.9, 50.0, 40.7, 39.4, 38.1, 37.9, 37.0, 36.7, 34.4, 32.8, 32.2, 32.0, 31.6, 30.8, 30.5, 30.1, 29.5, 29.4, 29.3, 29.2, 28.4, 27.7, 26.8, 25.0, 21.4, 20.6, 19.3, 18.9, 16.8, 16.4; HRESIMS:  $m/z$  778.5601  $[\text{M} + \text{Na}]^+$  (calcd for  $\text{C}_{46}\text{H}_{77}\text{NO}_7\text{Na}$ , 778.5598).

**4.2.3.3. General procedure for the synthesis of (25R)-furost-5-en-3 $\beta$ -acetoxy-26-yl amino acid esters 14–17.**  $\text{CF}_3\text{COOH}$  (10.0 mmol) was added to a stirred solution of **14a–17a** (0.5 mmol) in  $\text{CH}_2\text{Cl}_2$  (10 ml) at room temperature for 4–10 h. Then the mixture solution was removed *in vacuo* and purified by column chromatography ( $\text{CH}_2\text{Cl}_2/\text{CH}_3\text{OH}$  15:1), and then freeze-dried at  $-80^\circ\text{C}$  to yield **14–17**.

(25R)-Furost-5-en-3 $\beta$ -acetoxy-26-yl glycinate (**14**): yellowish viscous solid (92%);  $R_f = 0.40$  ( $\text{CH}_2\text{Cl}_2/\text{CH}_3\text{OH}/\text{CH}_3\text{COOH}$  6:1:0.1);  $^1\text{H}$  NMR (400 MHz,  $\text{CDCl}_3$ )  $\delta$  5.37 (d,  $J = 4.5$  Hz, 1H), 4.66–4.52 (m, 1H), 4.30 (dd,  $J = 13.0$ , 7.6 Hz, 1H), 4.11–4.02 (m, 1H), 4.01–3.92 (m, 1H), 3.80 (s, 2H), 3.38–3.22 (m, 1H), 2.32 (d,  $J = 6.4$  Hz, 2H), 2.03 (s, 3H), 1.03 (s, 3H), 0.99 (d,  $J = 6.6$  Hz, 3H), 0.91 (d,  $J = 6.6$  Hz, 3H), 0.80 (s, 3H);  $^{13}\text{C}$  NMR (100 MHz,  $\text{CDCl}_3$ )  $\delta$  170.6, 167.7, 139.7, 122.4, 90.0, 83.2, 73.9, 71.5, 65.0, 56.9, 50.0, 40.7, 39.4, 38.1, 37.9, 37.0, 36.7, 32.5, 32.2, 32.0, 31.6, 30.7, 30.2, 27.7, 21.4, 20.6, 19.3, 18.8, 16.4; HRESIMS:  $m/z$  516.3691  $[\text{M} + \text{H}]^+$  (calcd for  $\text{C}_{31}\text{H}_{50}\text{NO}_5$ , 516.3689).

(25R)-Furost-5-en-3 $\beta$ -acetoxy-26-yl 4-aminobutyrate (**15**): yellowish viscous solid (86%);  $R_f = 0.32$  ( $\text{CH}_2\text{Cl}_2/\text{CH}_3\text{OH}/\text{CH}_3\text{COOH}$  6:1:0.1);  $^1\text{H}$  NMR (400 MHz,  $\text{CDCl}_3$ )  $\delta$  5.37 (d,  $J = 4.6$  Hz, 1H), 4.68–4.52 (m, 1H), 4.30 (dd,  $J = 13.0$ , 7.6 Hz, 1H), 3.97 (dd,  $J = 11.2$ , 5.0 Hz, 1H), 3.85 (dd,  $J = 10.6$ , 7.0 Hz, 1H), 3.31 (td,  $J = 8.1$ , 4.0 Hz, 1H), 3.02 (s, 2H), 2.45 (t,  $J = 6.5$  Hz, 2H), 2.32 (d,  $J = 6.7$  Hz, 2H), 2.03 (s, 3H), 2.01–1.93 (m, 3H), 1.86 (d,  $J = 10.7$  Hz, 2H), 1.04 (s, 3H), 0.99 (d,  $J = 6.7$  Hz, 3H), 0.92 (d,  $J = 6.7$  Hz, 3H), 0.80 (s, 3H);  $^{13}\text{C}$  NMR (100 MHz,  $\text{CDCl}_3$ )  $\delta$  173.4, 170.6, 139.7, 122.4, 90.1, 83.2, 73.9, 70.0, 65.1, 56.9, 50.0, 40.7, 39.4, 38.1, 37.9, 37.0, 36.7, 32.7, 32.2, 32.0, 31.6, 31.1, 30.8, 30.4, 27.7, 22.3, 21.4, 20.6, 19.3, 18.9, 16.6, 16.4; HRESIMS:  $m/z$  544.4007  $[\text{M} + \text{H}]^+$  (calcd for  $\text{C}_{33}\text{H}_{54}\text{NO}_5$ , 544.4002).

(25R)-Furost-5-en-3 $\beta$ -acetoxy-26-yl 6-aminohexanoate (**16**): yellowish viscous solid (89%);  $R_f = 0.35$  ( $\text{CH}_2\text{Cl}_2/\text{CH}_3\text{OH}/\text{CH}_3\text{COOH}$  6:1:0.1);  $^1\text{H}$  NMR (400 MHz,  $\text{CDCl}_3$ )  $\delta$  5.37 (d,  $J = 4.7$  Hz, 1H), 4.60 (dt,  $J = 11.6$ , 6.7 Hz, 1H), 4.30 (dd,  $J = 13.0$ , 7.6 Hz, 1H), 3.96 (dd,  $J = 10.5$ , 5.4 Hz, 1H), 3.84 (dd,  $J = 10.7$ , 7.0 Hz, 1H), 3.31 (td,  $J = 8.1$ , 4.1 Hz, 1H), 2.94 (s, 2H), 2.31 (t,  $J = 7.1$  Hz, 4H), 2.03 (s, 3H), 2.02–1.95 (m, 2H), 1.86 (d,  $J = 10.6$  Hz, 2H), 1.04

(s, 3H), 0.99 (d,  $J = 6.7$  Hz, 3H), 0.92 (d,  $J = 6.7$  Hz, 3H), 0.80 (s, 3H);  $^{13}\text{C}$  NMR (100 MHz,  $\text{CDCl}_3$ )  $\delta$  174.0, 170.6, 139.7, 122.4, 90.2, 83.2, 73.9, 69.5, 65.1, 56.9, 50.0, 40.7, 39.8, 39.4, 38.1, 37.9, 37.0, 36.7, 33.7, 32.8, 32.2, 32.0, 31.6, 30.8, 30.4, 27.7, 26.9, 25.6, 24.0, 21.4, 20.6, 19.3, 18.9, 16.7, 16.4; HRESIMS:  $m/z$  572.4327  $[\text{M} + \text{H}]^+$  (calcd for  $\text{C}_{35}\text{H}_{58}\text{NO}_5$ , 572.4315).

(25*R*)-Furost-5-en-3 $\beta$ -acetoxy-26-yl 12-aminolaurate (**17**): yellowish viscous solid (90%);  $R_f = 0.42$  ( $\text{CH}_2\text{Cl}_2/\text{CH}_3\text{OH}/\text{CH}_3\text{COOH}$  6:1:0.1);  $^1\text{H}$  NMR (400 MHz,  $\text{CDCl}_3$ )  $\delta$  5.37 (d,  $J = 4.6$  Hz, 1H), 4.65–4.54 (m, 1H), 4.31 (dd,  $J = 13.0, 7.6$  Hz, 1H), 3.96 (dd,  $J = 10.6, 5.5$  Hz, 1H), 3.85 (dd,  $J = 10.7, 6.9$  Hz, 1H), 3.32 (td,  $J = 8.0, 4.2$  Hz, 1H), 2.91 (s, 2H), 2.30 (dd,  $J = 14.6, 7.2$  Hz, 4H), 2.03 (s, 3H), 1.04 (s, 3H), 1.00 (d,  $J = 6.7$  Hz, 3H), 0.93 (d,  $J = 6.7$  Hz, 3H), 0.80 (s, 3H);  $^{13}\text{C}$  NMR (100 MHz,  $\text{CDCl}_3$ )  $\delta$  174.3, 170.7, 139.7, 122.4, 90.2, 83.2, 74.0, 69.2, 65.1, 56.9, 50.0, 40.7, 40.2, 39.4, 38.1, 37.9, 37.0, 36.7, 34.4, 32.8, 32.2, 32.0, 31.6, 30.8, 30.4, 29.3, 29.2, 28.9, 27.7, 27.4, 26.2, 25.0, 21.4, 20.7, 19.3, 18.9, 16.8, 16.4; HRESIMS:  $m/z$  656.5258  $[\text{M} + \text{H}]^+$  (calcd for  $\text{C}_{41}\text{H}_{70}\text{NO}_5$ , 656.5254).

#### 4.2.4. Synthesis of (22 $\beta$ , 25*R*)-spirost-5-en-3 $\beta$ -yl *n*-butyrate (**21**)

*n*-Butyric anhydride (3 ml, 18 mmol) was added to a solution of diosgenin (829 mg, 2 mmol) in pyridine (5 mmol) and the resulting solution stirred at room temperature until absence of diosgenin (checked by TLC). Then the reaction mixture was poured into water and stirred vigorously to get a white precipitate. The residue was washed with brine, recrystallized in methane to afford a white needle solid **21**.

(22 $\beta$ , 25*R*)-Spirost-5-en-3 $\beta$ -yl *n*-butyrate (**21**): white needle solid (89%);  $R_f = 0.55$  (petroleum ether/EtOAc 8:1);  $^1\text{H}$  NMR (400 MHz,  $\text{CDCl}_3$ )  $\delta$  5.37 (d,  $J = 5.0$  Hz, 1H), 4.66–4.56 (m, 1H), 4.41 (dd,  $J = 14.9, 7.5$  Hz, 1H), 3.51–3.43 (m, 1H), 3.37 (t,  $J = 10.9$  Hz, 1H), 2.36–2.28 (m, 2H), 2.25 (t,  $J = 7.4$  Hz, 2H), 2.06–1.93 (m, 2H), 1.90–1.82 (m, 3H), 1.04 (s, 3H), 0.95 (dd,  $J = 14.5, 7.2$  Hz, 6H), 0.79 (t,  $J = 3.1$  Hz, 6H);  $^{13}\text{C}$  NMR (100 MHz,  $\text{CDCl}_3$ )  $\delta$  172.1, 138.7, 121.3, 108.2, 79.8, 72.6, 65.8, 61.1, 55.4, 48.9, 40.6, 39.2, 38.7, 37.1, 36.0, 35.7, 35.6, 31.0, 30.8, 30.4, 29.3, 27.8, 26.8, 19.8, 18.3, 17.5, 16.1, 15.3, 13.5, 12.6; HRESIMS:  $m/z$  507.3450  $[\text{M} + \text{Na}]^+$  (calcd for  $\text{C}_{31}\text{H}_{48}\text{O}_4\text{Na}$ , 507.3450).

#### 4.2.5. Synthesis of (22 $\beta$ , 25*R*)-spirost-5-en-3 $\beta$ -yl aliphatic esters (**22–24**)

**4.2.5.1. General procedure for the synthesis of (22 $\beta$ , 25*R*)-spirost-5-en-3 $\beta$ -yl aliphatic esters **22–24**.** Compound **1** (2.0 mmol), **22a–24a** (3.0 mmol) and DMAP (0.5 mmol) were stirred in anhydrous  $\text{CH}_2\text{Cl}_2$  (20 ml) for 10 min. A solution of EDC·HCl (3.0 mmol) in  $\text{CH}_2\text{Cl}_2$  (10 ml) was added dropwise under  $\text{N}_2$ . The mixture was left to stir for 2–6 h at 30–35 °C (checked by TLC). The reaction solution was washed with brine, saturated  $\text{NaHCO}_3$  solution and brine, dried over anhydrous  $\text{Na}_2\text{SO}_4$ , and then filtered and concentrated. The residue was purified by a silica gel column chromatography (petroleum ether/EtOAc 25:1–15:1) to give **22–24**.

(22 $\beta$ , 25*R*)-Spirost-5-en-3 $\beta$ -yl *n*-hexanoate (**22**): white needle solid (79%);  $R_f = 0.59$  (petroleum ether/EtOAc 8:1);  $^1\text{H}$  NMR (400 MHz,  $\text{CDCl}_3$ )  $\delta$  5.37 (d,  $J = 5.0$  Hz, 1H), 4.67–4.54 (m, 1H), 4.41 (dd,  $J = 14.9, 7.5$  Hz, 1H), 3.52–3.43 (m, 1H), 3.37 (t,  $J = 10.9$  Hz, 1H), 2.36–2.29 (m, 2H), 2.26 (t,  $J = 7.5$  Hz, 2H), 2.08–1.91 (m, 1H), 1.90–1.81 (m, 1H), 1.04 (s, 3H), 0.97 (d,  $J = 6.9$  Hz, 3H), 0.90 (t,  $J = 6.9$  Hz, 3H), 0.79 (t,  $J = 3.1$  Hz, 6H);  $^{13}\text{C}$  NMR (100 MHz,  $\text{CDCl}_3$ )  $\delta$  172.3, 138.8, 121.3, 108.2, 79.8, 72.6, 65.8, 61.1, 55.4, 48.9, 40.6, 39.2, 38.7, 37.1, 36.0, 35.7, 33.7, 31.0, 30.8, 30.4, 30.3, 29.3, 27.8, 26.8, 23.7, 21.3, 19.8, 18.3, 16.1, 15.3, 13.5, 12.9; HRESIMS:  $m/z$  513.3936  $[\text{M} + \text{H}]^+$  (calcd for  $\text{C}_{33}\text{H}_{53}\text{O}_4$ , 513.3944).

(22 $\beta$ , 25R)-Spirost-5-en-3 $\beta$ -yl *n*-octanoate (**23**): white needle solid (84%);  $R_f$  = 0.62 (petroleum ether/EtOAc 8:1);  $^1\text{H}$  NMR (400 MHz,  $\text{CDCl}_3$ )  $\delta$  5.37 (d,  $J$  = 5.0 Hz, 1H), 4.67–4.54 (m, 1H), 4.41 (dd,  $J$  = 15.0, 7.5 Hz, 1H), 3.51–3.44 (m, 1H), 3.37 (t,  $J$  = 10.9 Hz, 1H), 2.37–2.29 (m, 2H), 2.27 (t,  $J$  = 7.5 Hz, 2H), 2.06–1.93 (m, 2H), 1.86 (m, 3H), 1.04 (s, 3H), 0.97 (d,  $J$  = 6.9 Hz, 3H), 0.88 (t,  $J$  = 6.8 Hz, 3H), 0.79 (t,  $J$  = 3.1 Hz, 6H);  $^{13}\text{C}$  NMR (100 MHz,  $\text{CDCl}_3$ )  $\delta$  172.3, 138.8, 121.3, 108.3, 79.8, 72.6, 65.8, 61.1, 55.4, 48.9, 40.6, 39.2, 38.7, 37.1, 36.0, 35.7, 33.7, 31.0, 30.8, 30.7, 30.4, 29.3, 28.1, 27.9, 27.8, 26.8, 24.1, 21.6, 19.8, 18.3, 16.1, 15.3, 13.5, 13.1; HRESIMS:  $m/z$  563.4071  $[\text{M} + \text{Na}]^+$  (calcd for  $\text{C}_{35}\text{H}_{56}\text{O}_4\text{Na}$ , 563.4076).

(22 $\beta$ , 25R)-Spirost-5-en-3 $\beta$ -yl *n*-laurate (**24**): white needle solid (81%);  $R_f$  = 0.67 (petroleum ether/EtOAc 8:1);  $^1\text{H}$  NMR (400 MHz,  $\text{CDCl}_3$ )  $\delta$  5.37 (d,  $J$  = 5.0 Hz, 1H), 4.67–4.54 (m, 1H), 4.41 (dd,  $J$  = 14.9, 7.5 Hz, 1H), 3.51–3.44 (m, 1H), 3.37 (t,  $J$  = 10.9 Hz, 1H), 2.35–2.29 (m, 2H), 2.26 (t,  $J$  = 7.5 Hz, 2H), 2.08–1.94 (m, 2H), 1.92–1.81 (m, 3H), 1.04 (s, 3H), 0.97 (d,  $J$  = 6.9 Hz, 3H), 0.88 (t,  $J$  = 6.8 Hz, 3H), 0.79 (t,  $J$  = 3.1 Hz, 6H);  $^{13}\text{C}$  NMR (100 MHz,  $\text{CDCl}_3$ )  $\delta$  173.3, 139.8, 122.3, 109.3, 80.8, 73.6, 66.8, 62.1, 56.4, 50.0, 41.6, 40.3, 39.7, 38.1, 37.0, 36.7, 34.7, 32.1, 31.9, 31.4, 30.3, 29.6, 29.5, 29.3, 29.1, 28.8, 27.8, 25.1, 22.7, 20.8, 19.3, 17.1, 16.3, 14.5, 14.1; HRESIMS:  $m/z$  619.4697  $[\text{M} + \text{Na}]^+$  (calcd for  $\text{C}_{39}\text{H}_{64}\text{O}_4\text{Na}$ , 619.4702).

#### 4.2.6. Synthesis of (22 $\beta$ , 25R)-spirost-5-en-3 $\beta$ -yl *N*-4-(7-nitrobenz-2-oxa-1,3-diazole)-6-aminohexanoate (**28**)

4-Chloro-7-nitrobenz-2-oxa-1,3-diazole (NBD-Cl, 200 mg, 1 mmol) and  $\text{Et}_3\text{N}$  (140  $\mu\text{l}$ , 1 mmol) was stirred in anhydrous THF (30 ml) for 10 min. A solution of compound **4** (528 mg, 1 mmol) in THF (20 ml) was added to the mixture solution in 30 min. Then the reaction was stirred at 50  $^\circ\text{C}$  for 5 h until absence of compound **4**. Then the reaction mixture was filtered and the filtrate was concentrated *in vacuo*. The crude residue was purification by column chromatography (petroleum ether/EtOAc 5:1) to yield **28**.

(22 $\beta$ , 25R)-spirost-5-en-3 $\beta$ -yl *N*-4-(7-nitrobenz-2-oxa-1,3-diazole)-6-aminohexanoate (**28**): orange powder solid (66%);  $R_f$  = 0.40 (petroleum ether/EtOAc 3:2);  $^1\text{H}$  NMR (400 MHz,  $\text{CDCl}_3$ )  $\delta$  8.49 (d,  $J$  = 8.6 Hz, 1H), 6.45 (t,  $J$  = 4.8 Hz, 1H), 6.18 (d,  $J$  = 8.7 Hz, 1H), 5.36 (d,  $J$  = 4.8 Hz, 1H), 4.67–4.55 (m, 1H), 4.41 (dd,  $J$  = 15.0, 7.5 Hz, 1H), 3.53 (dd,  $J$  = 12.8, 6.6 Hz, 2H), 3.48 (dd,  $J$  = 11.0, 4.1 Hz, 1H), 3.38 (t,  $J$  = 10.9 Hz, 1H), 2.39–2.27 (m, 4H), 1.03 (s, 3H), 0.97 (d,  $J$  = 6.9 Hz, 3H), 0.79 (t,  $J$  = 3.1 Hz, 6H);  $^{13}\text{C}$  NMR (100 MHz,  $\text{CDCl}_3$ )  $\delta$  172.9, 144.3, 143.9, 139.6, 136.5, 123.9, 122.5, 109.3, 98.6, 80.8, 74.0, 66.8, 62.1, 56.4, 49.9, 43.7, 41.6, 40.3, 39.7, 38.1, 36.9, 36.7, 34.2, 32.0, 31.8, 31.4, 30.3, 28.8, 28.1, 27.8, 26.3, 24.3, 20.8, 19.3, 17.2, 16.3, 14.5; HRESIMS:  $m/z$  691.4066  $[\text{M} + \text{H}]^+$  (calcd for  $\text{C}_{39}\text{H}_{55}\text{N}_4\text{O}_6$ , 691.4071).

#### 4.2.7. Synthesis of (22 $\beta$ , 25R)-spirost-5-en-3 $\beta$ -yl *N*- $\alpha$ -[4-(7-nitrobenz-2-oxa-1,3-diazole)]-L-lysinate (**32**)

4.2.7.1. Synthesis of (22 $\beta$ , 25R)-spirost-5-en-3 $\beta$ -yl *N*- $\alpha$ -Fmoc-*N*- $\epsilon$ -Boc-L-lysinate (**29**). To a solution of compound **1** (829 mg, 2.0 mmol), *N*- $\alpha$ -Fmoc-*N*- $\epsilon$ -Boc-L-lysine (1.12 g, 2.4 mmol), 4-dimethylaminopyridine (DMAP, 49 mg, 0.4 mmol) *p*-toluenesulfonic acid (TsOH, 69 mg, 0.4 mmol) in dry  $\text{CH}_2\text{Cl}_2$  (40 ml), and EDC-HCl (466 mg, 3.0 mmol) in anhydrous  $\text{CH}_2\text{Cl}_2$  (10 ml) were added dropwise under  $\text{N}_2$  atmosphere at room temperature. The mixture was stirred vigorously for 18 h. The reaction mixture was washed with brine, saturated  $\text{NaHCO}_3$  solution and brine, dried over anhydrous  $\text{Na}_2\text{SO}_4$ , and then filtered and concentrated. The residue was purified by a silica gel column chromatography (petroleum ether : EtOAc = 10:1) to give **29** (1.47 g, 85%) as a white powder.  $R_f$  0.70 (petroleum ether

: ethyl acetate = 1:1);  $^1\text{H}$  NMR (400 MHz,  $\text{CDCl}_3$ )  $\delta$  7.76 (d,  $J = 7.5$  Hz, 2H), 7.63–7.57 (m, 2H), 7.40 (t,  $J = 7.4$  Hz, 2H), 7.31 (t,  $J = 7.4$  Hz, 2H), 5.42 (d,  $J = 7.8$  Hz, 1H), 5.38 (d,  $J = 3.9$  Hz, 1H), 4.74–4.52 (m, 2H), 4.45–4.28 (m, 4H), 4.23 (t,  $J = 7.0$  Hz, 1H), 3.47 (dd,  $J = 10.3, 3.4$  Hz, 1H), 3.37 (t,  $J = 10.9$  Hz, 1H), 3.11 (d,  $J = 5.1$  Hz, 2H), 2.37–2.21 (m, 3H), 2.06–1.92 (m, 2H), 1.91–1.80 (m, 4H), 1.03 (s, 3H), 0.97 (d,  $J = 6.9$  Hz, 3H), 0.79 (d,  $J = 4.7$  Hz, 6H);  $^{13}\text{C}$  NMR (100 MHz,  $\text{CDCl}_3$ )  $\delta$  171.9, 156.1, 156.0, 144.0, 143.8, 141.3, 139.6, 139.3, 127.7, 127.1, 125.1, 122.8, 120.0, 109.3, 80.8, 75.2, 67.0, 66.9, 62.1, 56.4, 53.9, 49.9, 47.2, 41.6, 40.3, 39.7, 38.0, 36.9, 36.7, 32.4, 32.0, 31.8, 31.4, 30.3, 29.7, 28.8, 28.4, 27.7, 22.8, 22.4, 20.8, 19.3, 17.2, 16.3, 14.5; HRESIMS:  $m/z$  865.5359  $[\text{M} + \text{H}]^+$  (calcd for  $\text{C}_{53}\text{H}_{73}\text{N}_2\text{O}_8$ , 865.5367).

**4.2.7.2. Synthesis of (22 $\beta$ , 25R)-spirost-5-en-3 $\beta$ -yl N- $\epsilon$ -Boc-L-lysinate (30).** Compound **29** (643 mg, 1.0 mmol) was dissolved in DMF (5 ml), and piperidine (1 ml) was added and stirred at room temperature for 3 h. Then the reaction mixture was concentrated *in vacuo* and the crude residue was purified by column chromatography ( $\text{CH}_2\text{Cl}_2$ : $\text{CH}_3\text{OH}$  25:1) to yield compound **30** (533 mg, 83%, light yellow solid).  $R_f$  0.55 ( $\text{CH}_2\text{Cl}_2$ : $\text{CH}_3\text{OH}$ : $\text{CH}_3\text{COOH} = 6:1:0.1$ );  $^1\text{H}$  NMR (400 MHz,  $\text{CDCl}_3$ )  $\delta$  5.37 (d,  $J = 3.2$  Hz, 1H), 4.79–4.57 (m, 1H), 4.41 (dd,  $J = 15.1, 7.2$  Hz, 1H), 3.86 (s, 1H), 3.65 (s, 1H), 3.47 (dd,  $J = 9.8, 3.6$  Hz, 1H), 3.37 (t,  $J = 10.9$  Hz, 2H), 3.21 (s, 1H), 3.10 (dd,  $J = 12.6, 7.0$  Hz, 2H), 2.71 (s, 1H), 2.47–2.23 (m, 5H), 2.07–1.92 (m, 2H), 1.03 (s, 3H), 0.98 (d,  $J = 6.9$  Hz, 3H), 0.79 (d,  $J = 4.2$  Hz, 6H); HRESIMS:  $m/z$  643.4689  $[\text{M} + \text{H}]^+$  (calcd for  $\text{C}_{38}\text{H}_{63}\text{N}_2\text{O}_6$ , 643.4686).

**4.2.7.3. Synthesis of (22 $\beta$ , 25R)-spirost-5-en-3 $\beta$ -yl N- $\alpha$ -[4-(7-nitrobenz-2-oxa-1,3-diazole)]-N- $\epsilon$ -Boc-L-lysinate (31).** NBD-Cl (100 mg, 0.5 mmol) and  $\text{Et}_3\text{N}$  (70  $\mu\text{l}$ ) were stirred in anhydrous THF (10 ml) for 10 min. A solution of compound **30** (257 mg, 0.4 mmol) in THF (10 ml) was added and the reaction was stirred at 50  $^\circ\text{C}$  for 4 h. The mixture solution was concentrated *in vacuo*. After the crude residue was re-dissolved in  $\text{CH}_2\text{Cl}_2$  (30 ml), the organic solution was washed with brine, dried over anhydrous  $\text{Na}_2\text{SO}_4$ , and then purified by flash chromatography. The purification by column chromatography (petroleum ether/ $\text{EtOAc}$  5:1) yielded **31** (238 mg, 74%, jacinth solid).  $R_f$  0.29 (petroleum ether/ $\text{EtOAc} = 2:1$ ); HRESIMS:  $m/z$  828.4566  $[\text{M} + \text{Na}]^+$  (calcd for  $\text{C}_{44}\text{H}_{63}\text{N}_5\text{O}_9\text{Na}$ , 828.4523).

**4.2.7.4. (22 $\beta$ , 25R)-Spirost-5-en-3 $\beta$ -yl N- $\alpha$ -[4-(7-nitrobenz-2-oxa-1,3-diazole)]-L-lysinate (32).** Trifluoroacetic acid ( $\text{CF}_3\text{COOH}$ , 0.3 ml, 4 mmol) was added to a solution of compound **31** (161 mg, 0.2 mmol) in  $\text{CH}_2\text{Cl}_2$  (10 ml) at room temperature and reacted at 30  $^\circ\text{C}$  for 4 h. Then the organic solution was concentrated and purified over silica gel column ( $\text{CH}_2\text{Cl}_2$ : $\text{CH}_3\text{OH} = 15:1$ ) to get compound **32** (124 mg, 88%, brownish red solid).  $R_f$  0.35 ( $\text{CH}_2\text{Cl}_2$ : $\text{CH}_3\text{OH}$ : $\text{CH}_3\text{COOH} = 6:1:0.1$ );  $^1\text{H}$  NMR (400 MHz,  $\text{CDCl}_3$ )  $\delta$  8.46 (d,  $J = 8.7$  Hz, 1H), 6.14 (d,  $J = 8.7$  Hz, 1H), 5.34 (d,  $J = 4.1$  Hz, 1H), 5.31 (s, 1H), 4.71–4.58 (m, 1H), 4.41 (dd,  $J = 15.0, 7.4$  Hz, 1H), 3.57–3.44 (m, 4H), 3.38 (t,  $J = 10.9$  Hz, 1H), 2.29 (d,  $J = 7.8$  Hz, 2H), 2.18 (d,  $J = 3.1$  Hz, 1H), 2.06–1.94 (m, 3H), 1.92–1.82 (m, 6H), 1.02 (s, 3H), 0.97 (d,  $J = 6.9$  Hz, 3H), 0.79 (t,  $J = 3.0$  Hz, 6H);  $^{13}\text{C}$  NMR (100 MHz,  $\text{CDCl}_3$ )  $\delta$  175.1, 144.3, 144.0, 139.3, 136.6, 123.4, 122.7, 109.3, 80.8, 74.7, 66.8, 62.1, 56.4, 54.0, 49.9, 41.6, 40.2, 39.7, 38.1, 36.9, 36.7, 33.6, 32.0, 31.8, 31.4, 30.3, 29.7, 29.3, 28.8, 27.7, 27.5, 23.1, 22.7, 20.8, 19.3, 17.2, 16.3, 14.5, 14.1; HRESIMS:  $m/z$  706.4281  $[\text{M} + \text{H}]^+$  (calcd for  $\text{C}_{39}\text{H}_{56}\text{N}_5\text{O}_7$ , 706.4180).

### **4.3. Biological evaluation**

#### **4.3.1. Cell culture**

Mouse colon carcinoma C26 cells, mouse melanoma B16 cells, human HepG2 cells, human lung carcinoma A549 cells, and human breast cancer MDA-MB-231 cells were maintained in RPMI 1640 medium or DMEM medium (Hyclone, Logan, USA) supplemented with 10% fetal bovine serum (Gibco, New York, USA). All experiments were performed in triplicate.

#### **4.3.2. Cytotoxicity evaluation**

Murine colon carcinoma C26 cells, mouse melanoma B16 cells, human hepatocellular carcinoma HepG2 cells, human lung carcinoma A549 cells, and human breast cancer MDA-MB-231 cells were plated at a density of  $3\text{--}5 \times 10^4$  cells/ml in 96-well plates, followed by stimulation of indicated concentrations of synthesized compounds, and carrier DMSO (<0.05%) was used as the vehicle control. After 24 h, cell viability was measured using MTT assay (Sigma-Aldrich, St. Louis., USA) according to the manufacturer's protocol. The absorbance at 490 nm was measured with VersaMax microplate reader (Molecular Devices, San Francisco, USA).

#### **4.3.3. Cellular localization imaging**

The cellular localization of diosgenyl derivatives in C26 cells was illustrated by fluorescent labeling assay. C26 cells were incubated with NBD-labeled compound **28** or **32** (10  $\mu$ M). After 24 h, cells were co-stained with 5  $\mu$ g/ml Hoechst 33342 (Invitrogen, Carlsbad, USA), and images were taken using a confocal laser scanning microscope (Nikon Eclipse Ti, Tokyo, Japan).

#### **4.3.4. Cell morphological analysis**

C26 cells were treated with indicated concentrations of compound **4** for 24 h, and then images were taken by inverted microscope Olympus IX71 (Olympus, Tokyo, Japan). To obtain the changes of subcellular structures, TEM was used. After 24 h treatment with vehicle or compound **4**, cells were then fixed in glutaraldehyde, osmicated with osmium tetroxide, dehydrated by graded ethanol, embedded in Epon-Araldite resin. Ultrathin sections were cut, double stained, and analyzed by H-600IV TEM (Hitachi, Tokyo, Japan).

#### **4.3.5. Colony formation assay**

C26 cells were plated at a density of 100 cells in culture dish (diameter 6 cm), followed by stimulation of compound **4** (0.625, 1.25, 2.5  $\mu$ M) for 7 days. Then cells were fixed with 4% paraformaldehyde, stained with 1% crystal violet and counted.

#### **4.3.6. Cell cycle analysis**

The effect of compound **4** on cell division cycle was assessed by flow cytometry with PI-stained cellular DNA as described earlier. Briefly, cells ( $4 \times 10^5$  per well) were seeded in 6-well culture plate and grown overnight. After exposure to compound **4** (0, 1.25, 2.5, 5  $\mu$ M) for 24 h, cells were harvested by trypsinization and fixed with ice-cold 70% ethanol overnight at 4 °C. The pellets were washed with PBS and resuspended in a solution containing PI (20 mg/ml), Triton X100 (0.1%) and RNase (1 mg/ml) in PBS. Then cell cycle was analyzed by Elite ESP flow cytometer (Beckman Coulter, High Wycombe, UK).

#### **4.3.7. Cytoplasmic Ca<sup>2+</sup> concentration analysis**

Cytoplasmic Ca<sup>2+</sup> concentration was measured using Fluo-4 AM (ThermoFisher Scientific, South San Francisco, USA) by flow cytometry. C26 cells were treated with compound **4** (0, 2.5, 5 μM) for 6 and 12 h, and then incubated with 5 μM Fluo-4 AM in HBSS for 30 min at 37 °C. Then cells were subjected to flow cytometer, and 20,000 cells were collected for the determination of fluorescence intensity of each sample.

#### **4.3.8. Mitochondrial membrane potential analysis**

Mitochondrial membrane potential was measured using JC-1 (ThermoFisher Scientific, South San Francisco, USA) by flow cytometry. C26 cells were treated with compound **4** (0, 2.5, 5 μM) for 6 and 12 h, and then incubated with 10 μg/ml JC-1 for 15 min at 37 °C. Then cells were subjected to flow cytometer, and 20,000 cells were collected for the determination of fluorescence intensity of each sample.

#### **4.3.9. ATP measurement**

Cellular ATP concentration was assessed as described previously. Cells were incubated with compound **4** (0, 2.5, 5 μM) for 6 and 12 h at 37 °C. Subsequently, cells were lysed, centrifuged, and the supernatant was transferred to a black opaque 96-well microplate (Corning, New York, USA). Cellular ATP levels were examined using an ATP Assay Kit (Invitrogen, Carlsbad, USA), and the values were expressed using untreated wells at 100%.

#### **4.3.10. Western blot analysis**

For apoptosis testing, C26 cells were serum-starved overnight and then incubated with compound **4** (0, 1.25, 2.5, 5 μM) for 24 h. For autophagy analysis, C26 cells were serum-starved overnight and then incubated with compound **4** (5 μM) for 0, 1, 2, 4 h. After treatment with compound **4**, cell lysates were subjected to SDS-PAGE on 10–15% gels followed by transfer to PVDF membrane. The membranes were incubated with antibodies against PARP and LC3 I/II (Cell Signaling Technology, Beverly, USA). GAPDH (Santa Cruz Biotechnology, Santa Cruz, USA) was used as whole-cell extract loading control. Primary antibodies were detected using either peroxidase-conjugated goat anti-rabbit IgG or peroxidase-conjugated goat anti-mouse IgG secondary antibody (Proteintech, Chicago, USA). The proteins were visualized with enhanced chemiluminescence detection (Amersham Biosciences, Sunnyvale, USA).

#### **4.3.11. Experimental animals**

All animal experiments were performed in accordance with the Guidelines for the Care and Use of Laboratory Animals and the Association for Research in Vision and Ophthalmology. All protocols were approved by the Institutional Animal Care and Use Committee of Sichuan University and the approval number for the animal experiments is 2014008B. Male BALB/c mice (4–6 weeks old) were obtained and supplied by Experimental Animal Research Center, West China School of Pharmacy, Sichuan University. The animals had free access to standard laboratory food and water, and housed at 22 ± 2 °C with a 12 h light/dark cycle. All surgeries were performed under anesthesia, and supplemental anesthesia was administered as needed. All efforts were made to minimize suffering and the number of animals used.

#### **4.3.12. Tumor xenograft model**

Mice were injected subcutaneously with C26 cells ( $1 \times 10^6$  cells per mouse) as previously described [19]. One week after cells implantation, the animals were randomly divided into three groups ( $n = 9$ ). Compound **4** (0, 15, 30 mg/kg) was administrated intraperitoneally every day for 28 days. Bodyweight and tumor growth were measured every 3 or 4 days. At the time of killing, tumor and main visceral organs were removed, frozen tumor tissues were used to detect the vessel density with an anti-CD31 antibody (BD Biosciences, San Jose, USA); and the main visceral organs were fixed in 10% formalin immediately, and H&E staining was performed.

#### **4.3.13. Bleeding time assay**

Mice tail bleeding time was measured as reported previously [11]. Male Balb/c mice were randomly divided into six groups of ten each. Before the bleeding time was assessed, the mice were given diosgenyl analogues **1**, **4**, **16**, and **22**, or control buffer orally (100  $\mu$ l) twice a day for five days. After 1 h for the last administration, mice were anesthetized intraperitoneally with pentobarbital sodium (40 mg/kg). Then an incision was made at the tip of the tail with a scalpel, and the tail was immersed immediately in saline (37 °C). The time from the incision to the cessation of bleeding was recorded, and a bleeding time of 900 s was used as the cut-off time for the purpose of statistical analysis. The measurement of bleeding time was performed in a blinded fashion.

#### **4.3.14. Particle size analysis**

Diosgenyl analogue **4** (5 mg) was dissolved in the ethanol (100  $\mu$ l), and then slowly added into deionized water (5 ml) under stirring. Thus some amphiphilic diosgenin analogues could self-assemble into nanoparticles in water. The particle size distribution of compound **4** (1 mg/ml in 2% ethanol–water solution) was investigated on a Nano-Particle Size Analyzer LB-550 (Horiba Ltd., Kyoto, Japan). Each sample was tested at least three times. The particle morphology of compound **4** in 2% ethanol–water solution was measured using TEM.

#### **4.3.15. Statistical analysis**

Statistical analysis was performed with unpaired two-tailed *t*-test using Graphpad Prism 5 (Graphpad Software, San Diego, USA) when two individual experimental groups were analyzed. For multiple comparisons, a one-way ANOVA with Dunnett's multiple comparison test was used. Values of \* $p < 0.05$  and \*\* $p < 0.01$  were considered significant. All data are represented as mean  $\pm$  s.e.m.

### **Acknowledgments**

We thank the study participants for their supports. The following are acknowledged for technical assistance: Yanyan Zhang and Zhihui Zhong for live cell imaging; Jie Zhang and Ling Bai for confocal microscope; Fang-Fang Wang and Fang-Fang Zhang for flow cytometer; Guang Yang for animal care; Jing-Yi Zhang for fluorescence microplate reader; Bin Zhou for chemiluminescence detection.

### **Disclosure statement**

No potential conflict of interest was reported by the authors.

## Funding

This work is supported in part by grants from China National “12.5” Research Foundation [grant number 2011BAJ07B04], National Natural Science Foundation of China [grant number 20972105] and Sichuan Province Research Foundation [grant number 2008SZ0024].

## References

- [1] X. Gao, S. Wang, B. Wang, S. Deng, X. Liu, X. Zhang, L. Luo, R. Fan, M. Xiang, C. You, Y. Wei, Z. Qian, and G. Guo, *Biomaterials*. **53**, 646 (2015).
- [2] A. Wicki, D. Witzigmann, V. Balasubramanian, and J. Huwyler, *J. Controlled Release*. **200**, 138 (2015).
- [3] D.L. Hanna, R.H. White, and T. Wun, *Crit. Rev. Oncol. Hematol.* **88**, 19 (2013).
- [4] C. Frere, P. Debourdeau, A. Hij, F. Cajfinger, M.N. Onan, L. Panicot-Dubois, C. Dubois, and D. Farge, *Semin. Oncol.* **41**, 319 (2014).
- [5] M. Franchini, C. Bonfanti, and G. Lippi, *Thromb. Res.* **135**, 777 (2015).
- [6] M.A. Fernández-Herrera, H. López-Muñoz, J.M.V. Hernández-Vázquez, M. López-Dávila, M.L. Escobar-Sánchez, L. Sánchez-Sánchez, B.M. Pinto, and J. Sandoval-Ramírez, *Bioorg. Med. Chem.* **18**, 2474 (2010).
- [7] A.A. Hamid, M. Hasanain, A. Singh, B. Bhukya, Omprakash, P.G. Vasudev, J. Sarkar, D. Chanda, F. Khan, O.O. Aiyelaagbe, and A.S. Negi, *Steroids*. **87**, 108 (2014).
- [8] B.B. Shingate, and B.G. Hazra, *Chem. Rev.* **114**, 6349 (2014).
- [9] K. Patel, M. Gadewar, V. Tahilyani, and D.K. Patel, *Nat. Prod. Bioprospect.* **2**, 46 (2013).
- [10] J. Raju, and R. Mehta, *Nutr. Cancer*. **61**, 27 (2009).
- [11] R. Zhang, B. Huang, D. Du, X. Guo, G. Xin, Z. Xing, Y. Liang, Y. Chen, Q. Chen, Y. He, and W. Huang, *Steroids*. **78**, 1064 (2013).
- [12] G. Gong, Y. Qin, and W. Huang, *Phytomedicine*. **18**, 458 (2011).
- [13] B. Huang, D. Du, R. Zhang, X. Wu, Z. Xing, Y. He, and W. Huang, *Bioorg. Med. Chem. Lett.* **22**, 7330 (2012).
- [14] C. Tohda, Y. Lee, Y. Goto, and I. Nemere, *Sci. Rep.* **3**, 3395 (2013).
- [15] C.H. Huang, D.Z. Liu, and T.R. Jan, *J. Nat. Prod.* **73**, 1033 (2010).
- [16] S. Selim, and S.A. Jaouni, *Nat. Prod. Res.* **29**, 1 (2015).
- [17] Q. Tong, Y. He, Q. Zhao, Y. Qing, W. Huang, and X. Wu, *Steroids*. **77**, 1219 (2012).
- [18] Q. Tong, Q. Zhao, Y. Qing, X. Hu, L. Jiang, and X. Wu, *Steroids*. **96**, 30 (2015).
- [19] Q. Tong, Y. Qing, Y. Wu, X. Hu, L. Jiang, and X. Wu, *Toxicol. Appl. Pharmacol.* **281**, 166 (2014).
- [20] S. Haldar, S. Kumar, S.P. Kolet, H.S. Patil, D. Kumar, and G.C. Kundu, *J. Org. Chem.* **78**, 10192 (2013).
- [21] C. Li, L. Dai, K. Liu, L. Deng, T. Pei, and J. Lei, *RSC Adv.* **5**, 74828 (2015).
- [22] C. Giorgi, A. Romagnoli, P. Pinton, and R. Rizzuto, *Curr. Mol. Med.* **8**, 119 (2008).
- [23] K.J. Peyton, X.M. Liu, Y. Yu, B. Yates, and W. Durante, *J. Pharmacol. Exp. Ther.* **342**, 827 (2012).
- [24] M.J. Hsieh, T.L. Tsai, Y.S. Hsieh, C.J. Wang, and H.L. Chiou, *Arch. Toxicol.* **87**, 1927 (2013).